



# Myrrh Essential Oil Improves DSS-Induced Colitis by Modulating the MAPK Signaling Pathway: In vitro and in vivo Studies

Tiantian Tang<sup>1,2,\*</sup>, Yujiao Wang<sup>1,2,\*</sup>, Taotao Li<sup>1,2,\*</sup>, Ding Liu<sup>1,2</sup> , Kai Yang<sup>1,2</sup>, Jing Sun<sup>1,2</sup> , Yajun Shi<sup>1,2</sup>, Dongyan Guo<sup>1,2</sup>, Junbo Zou<sup>1,2</sup>, Fengyun Bai<sup>3</sup>, Ying Sun<sup>3</sup>, Mei Wang<sup>1,2</sup>, Xiaofei Zhang<sup>1,2</sup>

<sup>1</sup>Key Laboratory of Basic and New Drug Research in Chinese Medicine, Shaanxi University of Chinese Medicine, Xianyang, Shaanxi, People's Republic of China; <sup>2</sup>Shaanxi Provincial University Engineering Research Center of Chinese Medicine Aromatic Industry, Shaanxi University of Chinese Medicine, Xianyang, Shaanxi, People's Republic of China; <sup>3</sup>Shaanxi Dongtai Pharmaceutical Co., Ltd., Xianyang, Shaanxi, People's Republic of China

\*These authors contributed equally to this work

Correspondence: Mei Wang; Xiaofei Zhang, Key Laboratory of Basic and New Drug Research in Chinese Medicine; Shaanxi Provincial University Engineering Research Center of Chinese Medicine Aromatic Industry, Shaanxi University of Chinese Medicine, Xianyang, Shaanxi, 712046, People's Republic of China, Email wangmei0708@163.com; 2051028@sntcm.edu.cn

**Objective:** To explore the mechanism and active components of the anti-colitis effects of myrrh essential oil (MEO).

**Methods:** In this study, we investigated the anti-inflammatory effects and molecular mechanisms of MEO on dextran sulfate sodium (DSS)-induced colitis with in vitro cell experiments, RNA-seq (RNA Sequencing), Weighted gene co-expression network analysis (WGCNA), combined with “weighting coefficient” network pharmacology, as and in vivo pharmacodynamic experiments. A 3% DSS solution was used to induce colitis in BALB/c mice and MEO was administered orally. We performed gas chromatography-mass spectrometry (GC-MS) analysis of the MEO components. The disease activity index (DAI) was evaluated by observing body weight, fecal characteristics, and blood in the stool of mice. The levels of inflammatory cytokines (TNF- $\alpha$  and IL-1 $\beta$ ) in mouse serum were measured using ELISA (Enzyme-linked immunosorbent assay) kits. Additionally, the expression of MAPK-related proteins (JNK, p-JNK, ERK, and p-ERK) in mouse colonic tissues was detected by Western blotting and immunohistochemistry.

**Results:** MEO (0.0625–0.125 $\mu$ g/g, p.o.) significantly inhibited the expression of the inflammatory mediator Nitric oxide (NO) in lipopolysaccharide (LPS)-induced RAW264.7 macrophages. After treatment, there was a significant increase in body weight and alleviation of diarrhea and bloody stools in colitis mice. It also reduced inflammatory cell infiltration. Furthermore, it decreased the serum levels of TNF- $\alpha$  and IL-1 $\beta$ , and reduced the activity of p-JNK and p-ERK in the MAPK pathway.

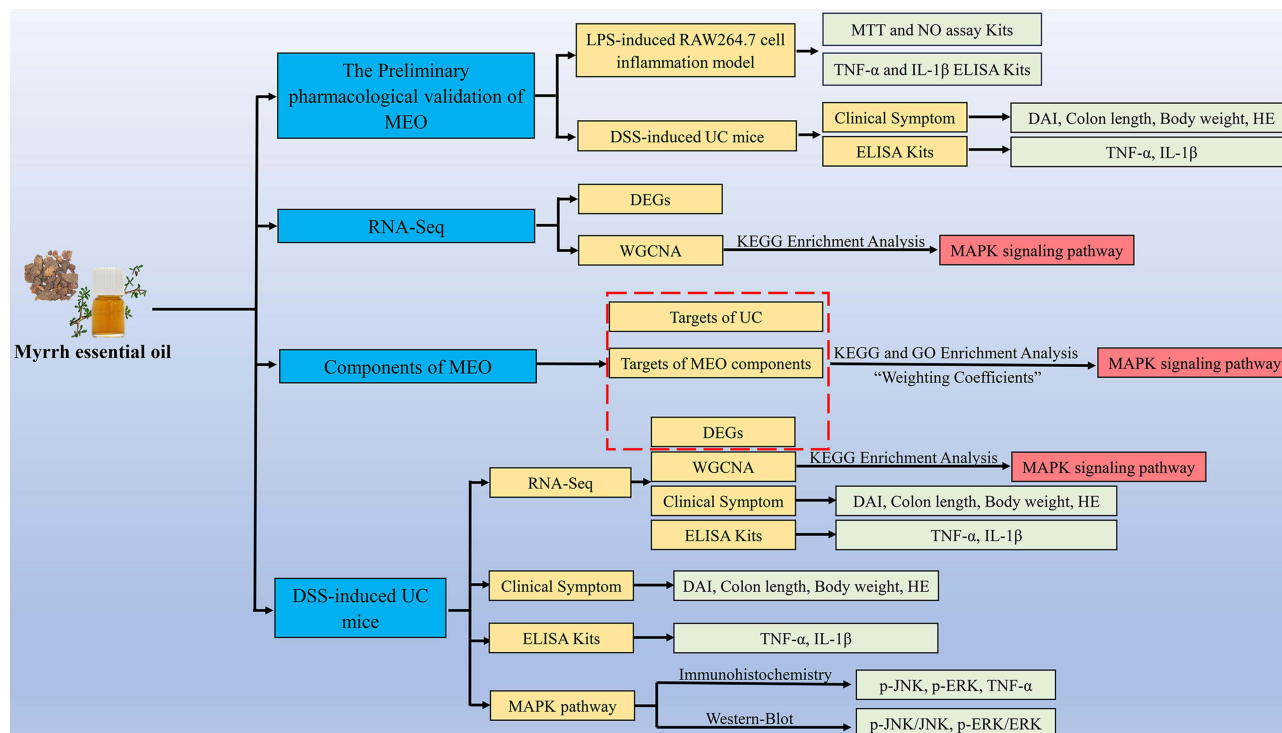
**Conclusion:** MEO relieved DSS-induced colitis by modulating the MAPK pathway. The experimental results indicate that the MAPK pathway might be inhibited by the synergistic effect of gamma-Murololene, Curzerene, beta-Elemene, and Furanouedesma 1.3-diene in MEO, which provides a novel idea for subsequent research and development of new anti-colitis drugs.

**Keywords:** colitis, myrrh essential oil, MAPK signaling pathway, RNA sequencing, weighted gene co-expression network analysis

## Introduction

Colitis is a nonspecific chronic inflammatory disease of the intestine with a high rate of recurrence and cancer of the digestive system.<sup>1</sup> Patients with colitis mainly present with symptoms such as diarrhea, mucus in stool, pus, and blood in stool.<sup>2</sup> Some studies have reported that approximately 30% of colitis require colectomy.<sup>3</sup> Most of the clinical drugs currently used to alleviate the symptoms of colitis are salicylic acid agents, immunosuppressive agents, and biological agents. However, these drugs generally have many adverse effects, leading to easy disease recurrence, are costly, and have poor patient compliance.<sup>4</sup> Currently, the research value of “aromatherapy”, which uses essential oil extracts from aromatic plants for therapeutic purposes, is increasing in medicine because of the anti-inflammatory, antibacterial, and

## Graphical Abstract



antioxidant effects of plant-based oil.<sup>5</sup> Therefore, in this study, we considered aromatherapy a potential therapeutic approach for treating colitis.

Myrrh (*Commiphora myrrha*), obtained from trees or shrubs of the genus *Commiphora* (*Burseraceae*), is an aromatic oleogum resin.<sup>6</sup> The chemical composition of myrrh is complex and diverse, mainly including resin, gum, essential oil, salts and acids,<sup>7</sup> among which essential oil is the characteristic component of myrrh, and is the basic substance that plays the pharmacological function and fragrance in myrrh.<sup>8</sup> Its components are complex and have significant anti-inflammatory and analgesic effects.<sup>9,10</sup> Myrrh essential oil (MEO) contains active components including Germacrene,<sup>11</sup> Elemene, Lindestrene, Furanocalypt-1,3-diene<sup>12</sup> and Curzerene. These components have anti-inflammatory,<sup>13</sup> analgesic<sup>14</sup> and immunostimulatory<sup>15</sup> effects; therefore, they are commonly used to treat inflammatory and infectious diseases.<sup>16</sup> Holleran reported that myrrh can reduce tumor necrosis factor (TNF)- $\alpha$  and interleukin (IL)-1 $\beta$  in the colon,<sup>17</sup> but its mechanism of action is not clear. Thus, in this study, we explored the mechanisms of action of MEO components in the treatment of colitis.

RNA Sequencing (RNA-seq) is commonly used to study possible changes in human disease-associated gene expression changes.<sup>18</sup> However, there are no studies related to the transcriptome sequencing of MEO for treating mice with DSS-induced colitis. Thus, we used a transcriptomic approach to explore the mechanism of action of MEO in the treatment of colitis. Traditional network pharmacology neglects the effect of component content,<sup>19</sup> therefore, we used weighting coefficients combined with network pharmacology to reduce the effect of content differences in drug components by weighting the drug components and their corresponding oral bioavailability (OB) as two key indicators to explore the mechanisms of action of drugs. Weighted gene co-expression network analysis (WGCNA) constructs gene co-expression networks between genes and phenotypes and clusters them according to gene expression for each sample,<sup>20</sup> obtaining important modules that are highly correlated with clinical traits and screening hub genes to explore the molecular mechanism of colitis.<sup>21</sup>

We based on in vitro cell experiments, MEO was used to treat LPS-induced RAW264.7 macrophages to observe its therapeutic effects. In addition, using animal experiments, analysis of RNA-seq, WGCNA, and weighting coefficients combined with network pharmacology and pharmacodynamic verification, we investigated the mechanisms of action of orally administered MEO in DSS-induced colitis mice.

## Materials and Methods

### Analysis and Identification of the Components of MEO

#### Gas Chromatography–Mass Spectrometry (GC–MS) Analysis of MEO

MEO (extracted from dried resin of *Commiphora molmol* in Somalia, Africa, LOT. 20210220) was purchased from Poli Aromatic Pharmaceutical Technology Co. Ltd. (Shanghai, China). The components in MEO were identified via GC-MS analysis. The GC-MS analysis utilized an HP5-MS column; the carrier gas was high-purity He, shunt ratio was set to 15:1, and injection volume was 1  $\mu$ L. The temperature of the inlet port was 260  $^{\circ}$ C, and a programmed temperature increase was used, with an initial temperature of 90  $^{\circ}$ C, an increase to 175  $^{\circ}$ C (rate 2  $^{\circ}$ C/min), and a hold for 5 min, followed by an increase to 210  $^{\circ}$ C (rate 1  $^{\circ}$ C/min), and a hold for 10 min. The mass range of the MS was 35–400 amu, the ionization source was EI, and ion source temperature was 230  $^{\circ}$ C.

#### MEO Components Identification

GC-MS results were analyzed using Data Analysis software and compared with the NIST database. MEO components were screened according to their matching degree, retention index (RI), and corresponding literature. Formula for the RI<sup>19</sup> is shown below (1–1):

$$RI = 100n + 100[t_r(M) - t_r(n)]/[t_r(n+1) - t_r(n)] \quad (1 - 1)$$

where  $t_r$  is the retention time, M is the compound to be analyzed, and n and n + 1 are the number of carbon atoms in two adjacent n-alkanes before and after the analyte, respectively, such that  $t_r(n) < t_r(M) < t_r(n+1)$ .

### Cell Culture

Complete culture medium was prepared by adding 10% Fetal Bovine Serum (FBS) and 1% penicillin-streptomycin to Dulbecco's modified Eagle's medium (DMEM) and mixing well. RAW264.7 macrophages (Procell Life Science&Technology Co., Ltd., Wuhan, China) were cultured in complete culture medium and incubated in a cell culture incubator (37  $^{\circ}$ C, 5% CO<sub>2</sub>).<sup>22</sup>

#### 3-(4,5-Dimethylthiazol-2-Yl)-2,5-Diphenyl Tetrazolium Bromide (MTT) Assay to Detect the Effect of MEO on the Viability of RAW264.7 Macrophages

The RAW264.7 cell density was adjusted to  $2 \times 10^5$ /mL, seeded at 100  $\mu$ L per well in 96-well plates, and incubated in a cell culture incubator (37  $^{\circ}$ C, 5% CO<sub>2</sub>). After 12 h, the culture medium was discarded, and different concentrations of MEO (0.0625, 0.125, 0.25, 0.5, and 1  $\mu$ g/g) were added to each well, and five replicate wells were set per concentration. The blank and control groups were established with five replicate wells for each group. Following the instructions of the MTT assay kit, the optical density (OD) value was measured at 490 nm with microplate reader (FC, Thermo Fisher Scientific Co., Ltd, Shanghai, China), and the cell viability was calculated to determine the optimal concentration. The calculation formula is as follows (1–2):

$$Cell\ viability = (m - a)/(n - a) \quad (1 - 2)$$

where a is the mean OD of the blank wells, m is the mean OD of the measurement wells, and n is the mean OD of the control wells.

#### The Levels of Nitric Oxide (NO), TNF- $\alpha$ and IL-1 $\beta$ in RAW264.7 Macrophages

##### Establishment of Cell Inflammation Model

The cell concentration was set at  $2 \times 10^6$ /mL, 100  $\mu$ L per well was seeded in 96-well plates, and put it in at 37  $^{\circ}$ C, 5% CO<sub>2</sub> incubator and incubate overnight. Different concentrations of MEO (0.0625, 0.125, and 0.25  $\mu$ g/g) were added to

each well, and five replicate wells were set for each concentration. After 1 hour, 1 µg/mL of Lipopolysaccharides (LPS) was added and incubated overnight to measure the levels of inflammatory factors.<sup>23</sup>

### Assay of NO

The NO assay kit was used according to the manufacturer's instructions. The cell supernatants (100 µL) were collected and operated according to the manufacturer's instructions, incubated for 15 min, and the OD value was measured at 550 nm using a microplate reader.

The calculation formula is as follows (1–3):

$$NO\ content(\mu mol/L) = (b - a)/(c - a) \times d \times N \quad (1 - 3)$$

where, a is the OD value of the blank wells, b is the OD value of the measurement wells, c is the OD value of the standard wells, d is the concentration of the standard (20 µmol/L), and N is the dilution time (four times).

### Determinations of TNF-α and IL-1β

The cell inflammation model was established according to 2.2.2.1 Establishment of cell inflammation model. The cell culture medium was collected in sterile tubes and centrifuged at 2500 rpm for 20 min, and the supernatants were collected. Following the instructions of the TNF-α and IL-1β Enzyme-linked immunosorbent assay (ELISA) kits, the OD value was measured at 450 nm using a microplate reader.

## Establishment of the Colitis Mice Model

Specific-pathogen-free (SPF) BALB/c male mice (Chengdu Dashuo Laboratory Animal Co., Ltd., Chengdu, China), weighing 18–22 g and animal license SCXK(Chuan)2020–030. Constant temperature, pressure, and acclimatization for one week. Animal experiments were approved by the Animal Ethics Committee of Shaanxi University of Traditional Chinese Medicine, Xianyang, China (Number: SUCMDC20220530003). The mice were divided into the following four groups (10 mice per group) according to the random number table method: control, model, positive, and MEO groups. The control group was administered drinking water only; the other groups were administered MP Biomedicals 3% dextran sulfate sodium (DSS) (lot number:0216011050) solution instead of water to induce colitis. Drug administration was started on the second day of modeling. Rapeseed oil, purchased from Sichuan Guanghan Oil & Grease Co., Ltd. (Sichuan, China) was gavaged at 0.01 mL/g/body weight in the control group. Mesalazine, purchased from Shanghai Ethypharm Pharmaceutical Co., Ltd. (Shanghai, China) was gavaged at 0.01 mL/g/body weight in the positive group. Rapeseed oil as a carrier for MEO was gavaged at 0.01 mL/g/body weight in the MEO (7.5 mg/kg) groups, and the body weight of the mice was measured daily for 7 days. The disease activity index (DAI) scores were calculated (Table 1).<sup>24</sup> At the end of the final administration, the mice were subjected to fasting without water for 24 h. Mice were anesthetized with isoflurane and blood was collected from their eyes. The blood samples were centrifuged (4 °C, 4000 rpm) for 10 min to obtain serum, which was then divided and stored at –20 °C. The mice were euthanized, their colons were dissected, and their natural lengths were recorded.<sup>25</sup> One part of the colon was fixed using paraformaldehyde, and the other parts were stored at –80 °C after quick-freezing in liquid nitrogen.<sup>26,27</sup>

**Table 1** Disease Activity Index (DAI) Score Table

Score	Weight Loss Rate (%)	Stool Consistency	Blood in Stool
0	0	Normal	Negative
1	1–5	Loose stool	Positive
2	6–10		
3	11–15	Diarrhea	Rectal bleeding
4	15		



## ELISA in Colitis Mice

TNF- $\alpha$  (MM-0132M1, Jiangsu Meimian Industrial Co., Ltd., Yancheng, China) and IL-1 $\beta$  (MM-0040M1, Jiangsu Meimian Industrial Co., Ltd., Yancheng, China) levels in the mouse serum were determined by ELISA. The assays were performed according to the manufacturer's instructions.

## Transcriptome Sequencing of the Colon Tissues of Mice

Total RNA was extracted from the colon tissues, which were stored at  $-80^{\circ}\text{C}$ , of three mice each in the control, model, and MEO groups, and poly(A)-mRNAs were purified. The purified mRNAs were fragmented and reverse-transcribed into double-stranded cDNA, followed by preparation of a double-stranded cDNA library.<sup>28</sup> Data analyses were performed using the Omicsmart (<https://www.omicsmart.com>) application platform with DESeq2 to identify differentially expressed genes (DEG). Gene Ontology (GO) and Kyoto Encyclopedia of Genes and Genomes (KEGG) pathway enrichment analyses were performed.

## WGCNA Analysis

Scale-free networks were constructed based on scale-free topology criteria for differential genes. The dynamic segmentation method was used to identify modules, a correlation analysis of all modules was carried out in pairs, and a heat map was drawn. Correlation analysis was also performed between the expression of each gene and the module eigenvalue. The TNF- $\alpha$  and IL- $\beta$  data of the correlation groups were established as trait files and correlation analysis was performed using module characteristic values. The modules most correlated with traits and phenotypes were used as target modules for the KEGG enrichment analysis.

## Component–Target Network Pharmacological Analyses

### Acquisition of MEO Components and Colitis Targets

PubChem (<https://pubchem.ncbi.nlm.nih.gov>), Index-Calcnet-TargetNet ([http://targetnet.scbdd.com/calcnet/calc\\_text](http://targetnet.scbdd.com/calcnet/calc_text)), and Swiss Target Prediction (<http://swisstargetprediction.ch>) databases were used to identify the relevant active component targets. GeneCards (<https://www.genecards.org>), Online Mendelian Inheritance in Man (OMIM, <https://omim.org>), DisGeNET (<https://www.disgenet.org>), and Comparative Toxicogenomics Database (CTD, <http://ctdbase.org>) databases were used to search for the term “colitis” to obtain relevant colitis targets, and duplicate targets were removed.

### Constructing Component–Target–Disease Interaction and Protein–Protein Interaction (PPI) Network

In the Venny 2.1.0 (<https://bioinfogp.cnb.csic.es/tools/venny>) platform, the intersection targets of “MEO-related component targets”, “colitis targets”, and “differential gene targets” was obtained and visualized in Cytoscape 3.7.1. The network for “active components-critical target” was constructed using the “differential gene targets” and imported into Cytoscape 3.7.1. The aforementioned intersection targets were imported into the STRING (<https://cn.string-db.org>) database,<sup>29</sup> the source was selected as “Homo sapiens” and adjusted the confidence to hide the free proteins in the network. The PPI results were visualized using Cytoscape 3.7.1. The PPI network was constructed using the key targets, with topological parameter  $\text{degree} > \text{averaged degree values of each node}$ .

### Establishing the Weighting Coefficients

MEO extracted from different herbs or purchased from different manufacturers can differ greatly in the content of the active components and their corresponding OBs. OB is crucial for measuring the pharmacokinetic processes and drug-forming properties of drugs. Therefore, we multiplied the relative content of MEO components by their OBs to obtain the weighting coefficient. The weighting coefficient (T) and weighting coefficients were calculated as follows:

$$T = w \times OB \quad (1 - 4)$$

where  $w$  denotes the relative content of each component;

$$A = \sum_{i=1}^n T_i \quad (1 - 5)$$

where A denotes the weight coefficient of each target and  $T_i$  denotes the weighting coefficient of each component included in A.

$$B = \sum_{i=1}^n A_i \quad (1 - 6)$$

where B denotes the weighting coefficient of each pathway and  $A_i$  denotes the weight coefficient of each target included in B.

### GO and KEGG Pathway Enrichment Analyses

The intersected targets under 1.5.2 were analysed by GO and KEGG using the “clusterProfiler<sup>30</sup>”, “org.Hs.eg.db<sup>31</sup>”, and “ggplot2<sup>32</sup>” packages in R to obtain the pathway ranking results. The enriched pathway entries were ranked based on their weighting coefficients.

### Molecular Docking

Molecular docking was performed for the key targets CACN, RAS, ERK, and JNK, which were obtained by pathway enrichment. The 3D protein structures were downloaded from the PCSB-PDB (<https://www.rcsb.org>) database.<sup>33</sup> Specific ligands corresponding to key targets were obtained from the DrugBank database (<https://go.drugbank.com/>), and the 2D structures of the components and specific ligands were downloaded from the PubChem database. We imported the 3D structure of the key target protein as receptors and the 2D structure of the MEO components and the specific ligands as ligands into Discovery Studio (DS) v4.0. The LibDock module<sup>34</sup> was used for docking and energy calculations.

## Pharmacodynamic Tests

### Animal Grouping and Establishment of the Colitis Mice Model

The strains, suppliers and feeding environment of mice was the same as under 2.3 Establishment of colitis mice model. The difference, however, was that BALB/c mice were divided into the following six groups (10 mice per group) based on the random number table method: control, model, positive group, and low-dose, medium-dose, high-dose MEO group. The control group was administered only drinking water, whereas the other groups were administered a 3% DSS solution instead of drinking water to induce colitis. Drug administration was started on the second day of modeling. The control group was gavaged with rapeseed oil at 0.01 mL/g. On the other hand, the low- (3.75 mg/kg), medium- (7.5 mg/kg), and high- (15 mg/kg) dose MEO groups were gavaged with MEO in rapeseed oil at 0.01 mL/g for 7 days and calculated DAI score.

### Biological Sample Collection and Processing

At the end of the final administration, the biological sample collection and processing was performed according to the procedure mentioned in 2.3 Establishment of colitis mice model.

### TNF- $\alpha$ and IL-1 $\beta$ ELISA Assays

ELISA was performed to determine the levels of TNF- $\alpha$  (MM-0132M1) and IL-1 $\beta$  (MM-0040M1) according to the procedure described in 2.3.1 ELISA in colitis mice.

### Hematoxylin-Eosin (HE) Staining

Colonic tissues of each group of mice were collected, dehydrated using an ethanol gradient, and embedded in paraffin. The tissues were stained with hematoxylin, restained with eosin, dehydrated to transparency, and sealed.

### Immunohistochemistry

Colon tissues of each mouse group were fixed in 4% paraformaldehyde, washed, dehydrated, immersed in wax, embedded, and sectioned. After dewaxing with xylene, samples were hydrated using an ethanol gradient. Nonimmune normal sheep serum was added to remove nonspecific antigens and the samples were washed with PBS. Then, Primary antibodies were added and the samples were incubated overnight at 4 °C. The following day, samples were incubated at room temperature for 40 min and washed again with PBS. Thereafter, horseradish peroxidase (HRP)-labeled secondary

antibodies (rabbit antibodies) were added, and the samples were incubated for 1 h at 37 °C, then washed again with PBS, stained with DAB, restained with hematoxylin, dehydrated using an ethanol gradient, and blocked with xylene after transparent treatment.<sup>35</sup>

Based on relevant research showing that TNF- $\alpha$  is a pro-inflammatory cytokine produced by various cell types and an important mediator in the inflammatory response and host defence,<sup>36</sup> involved in the regulation of the immune system, cell survival signaling pathways, proliferation and regulation of metabolic processes.<sup>37</sup> When the level of TNF- $\alpha$  in the body exceeds the normal level, it will disrupt the immune homeostasis of the body, induce and promote the production and release of other inflammatory mediators, amplify the level of inflammatory cascade response, and cause colitis. Cui et al<sup>38</sup> detected the expression of TNF- $\alpha$  in DSS-induced colitis mice by immunohistochemistry and found to be highly expressed in the DSS group, whereas TNF- $\alpha$  levels were significantly reduced after administration of resveratrol treatment. When colitis occurs, inflammation cytokines such as TNF- $\alpha$ , IL-1 and IL-6 can cause intestinal fibroblasts,<sup>39</sup> neutrophils and macrophages accumulate in the intestines, where fibroblasts will cause intestinal stenosis in patients with colitis. In addition to this, there are several pieces of evidence that TNF- $\alpha$  is associated with both human IBD and murine colitis.<sup>40–43</sup> Therefore, we considered using immunohistochemistry to detect the level of inflammatory factor TNF- $\alpha$  in colonic tissues after DSS induction.

### Western Blot

The colonic tissues of three mice from each group were weighed. A mixture of RIPA lysate and protease inhibitor was added and the samples were homogenized using a high-speed homogenizer and centrifuged at 4 °C for 5 min at 12000 rpm. Serum protein concentration was measured using a BCA kit.<sup>44</sup> Electrophoresis was performed on a sodium dodecyl sulfate-polyacrylamide gel, and at the end of the gel, the proteins were transferred to a PVDF membrane and blocked with 5% skim milk for 1 h. Added the Primary antibodies phosphorylated amino-terminal protein kinase (p-JNK) (Triple Eagle, 1:1000), c-Jun amino-terminal kinase (JNK) (Triple Eagle, 1:3000), phosphorylated extracellular signal-regulated kinase (p-ERK) (Saville, 1:400), and extracellular signal-regulated kinase (ERK) (Abcam, 1:1000), and the internal reference glyceraldehyde-3-phosphate dehydrogenase (GAPDH) (Huaan Bio, 1:5000) then incubated overnight at 4 °C. The membranes were then washed three times with TBST at room temperature, followed by the addition of HRP-labeled secondary antibodies (Jackson, 1:5000), incubated for 30 min at room temperature, washed with TBST, and developed using an ELC chromogen. Proteins were visualized using an imager<sup>45</sup> and the relative levels of the target proteins were calculated.

### Statistical Analysis

GraphPad Prism 9.0.0 software was used to statistically analyse all data. One-way analysis of variance was used to compare differences among the groups.  $P < 0.05$  was considered statistically different.

## Results

### Results of Analysis and Identification of MEO Components

The ion mass spectra of MEO are shown in [Figure 1A](#), and the data were matched with the NIST database, and 23 active components were screened based on their matching degree. The specific components are listed in [Table 2](#). The structures of the components are shown in [Figure 1B](#).

### The Anti-Inflammatory Effect of MEO on RAW264.7 Macrophages

#### Effect of MEO on Cell Viability

As shown in [Figure 2A](#), when the concentration of MEO was 0.0625, 0.125, and 0.25  $\mu\text{g/g}$ , the cell survival rate was above 95%, indicating no adverse effect on cell viability. Therefore, the selected concentrations were used for NO, TNF- $\alpha$ , and IL-1 $\beta$  experiments.

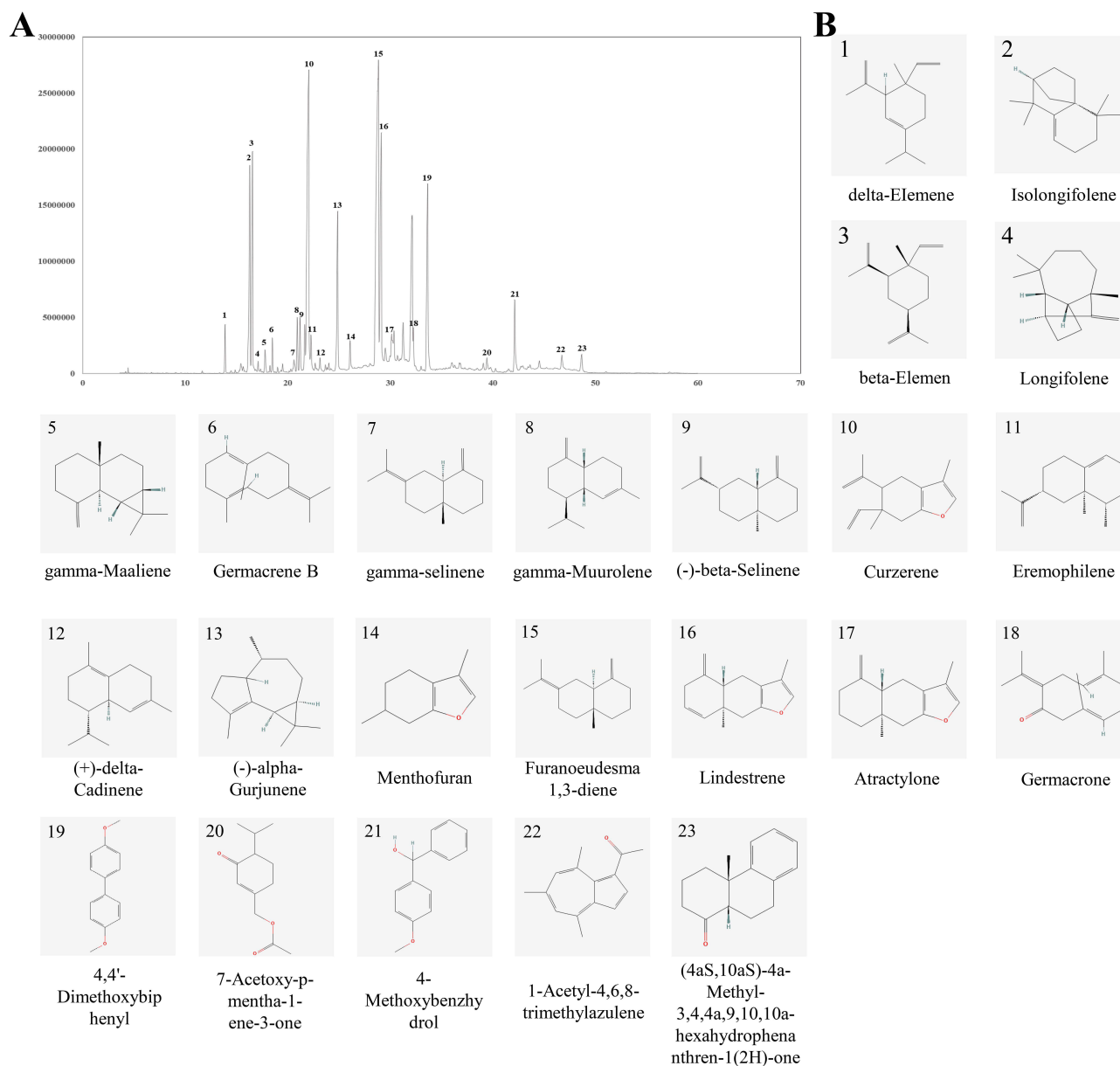


**Figure 1** GC-MS chromatogram of MEO and the structure of its components. **(A)** Total ion flow map of MEO. **(B)** Structures of 23 components in MEO.

### Effect of MEO on the Levels of NO, TNF- $\alpha$ , and IL-1 $\beta$ in LPS-Induced RAW264.7 Macrophages

As shown in **Figure 2B** and **D**, compared with the control group, the NO, TNF- $\alpha$ , and IL-1 $\beta$  levels in the cells of the model group were significantly higher ( $P < 0.01$ ). Compared to the model group, the levels of NO, TNF- $\alpha$ , and IL-1 $\beta$  at the three concentrations of MEO were significantly decreased ( $P < 0.01$ ).

### DAI, Colon Morphology and Serum Levels of TNF- $\alpha$ and IL-1 $\beta$ in Colitis Mice

The body weight of mice in the control group gradually increased. The model and MEO groups of mice had diluted feces on the third day with severe weight loss after modeling and blood in stool on the fourth day. However, the MEO group showed a gradual increase in body weight starting on day 5 and improved stool properties. **Figure 3A** and **B** illustrates the changes in DAI scores and body weights of the mice in each group. Images of the colon of each mouse group are shown in **Figure 3C**, and the differences in colon length are shown in **Figure 3D**. We observed that the colons of mice in the

**Table 2** Qualitative Results of the Components in MEO by GC-MS

NO.	Library/ID	CAS	RI	Pct Total
1	delta-Elemene	20307-84-0	1337.92	0.996
2	Isolongifolene	1135-66-6	1389.59	6.598
3	beta-Elemene	515-13-9	1395.23	7.715
4	Longifolene	475-20-7	1406.41	0.219
5	gamma-Maaliene	20071-49-2	1419.55	0.690
6	Germacrene B	15423-57-1	1433.49	0.778
7	gamma-Selinene	515-17-3	1474.52	1.861
8	gamma-Murolene	30021-74-0	1480.76	1.944
9	(-)-beta-Selinene	17066-67-0	1485.89	1.519
10	Curzerene	17910-09-7	1502.49	17.028
11	Eremophilene	10219-75-7	1506.70	1.097
12	(+)-delta-Cadinene	483-76-1	1523.24	0.390
13	(-)-alpha-Gurjunene	489-40-7	1555.85	5.202
14	Menthofuran	494-90-6	1578.94	0.843
15	Furanoedesma 1.3-diene	87605-93-4	1577.92	21.984
16	Lindestrene	2221-88-7	1578.78	9.223
17	Atractylone	6989-21-5	1581.87	8.894
18	Germacrone	6902-91-6	1588.42	0.705
19	4,4'-Dimethoxybiphenyl	2132-80-1	1670.73	7.488
20	7-Acetoxy-p-mentha-1-ene-3-one	56248-42-1	1766.74	0.360
21	4-Methoxybenzhydrol	720-44-5	1773.14	2.382
22	1-Acetyl-4,6,8-trimethylazulene	834-97-9	1866.13	0.518
23	(4aS,10aS)-4a-Methyl-3,4,4a,9,10,10a-hexahydrophenanthren-1(2H)-one	62318-99-4	1952.31	0.752

MEO group were longer and showed no mucosal congestion or swelling. Therefore, MEO effectively relieved colitis in mice.

The serum TNF- $\alpha$  and IL-1 $\beta$  levels were significantly higher in the model group ( $P < 0.0001$ ). In contrast, the levels of TNF- $\alpha$  and IL-1 $\beta$  in the MEO group decreased to different degrees ( $P < 0.001$ ). The results are shown in [Figure 3E](#) and [F](#).

## Results of RNA-Seq in Colitis Mice

Sequencing results were analyzed using the Omicsmart platform. The parameters were set as follows: false discovery rate (FDR)  $\leq 0.05$ ,  $|\log_2FC| = 1$ . Detected DEGs 3021 A total of 1688 upregulated and 1333 downregulated genes. The sample clustering (PCA) plot is shown in [Figure 4A](#), differential gene volcano plot is shown in [Figure 4B](#), and differential gene heat map is shown in [Figure 4C](#). KEGG and GO enrichment analyses of the identified DEGs were performed. As shown in [Figure 4D](#), 388 KEGG pathways were enriched, including the MAPK, PI3K-Akt, and P53 signaling pathway. The GO enrichment results are shown in [Figure 4E](#).

## WGCNA Analysis Results

A scale-free network with a soft threshold of eight is shown in [Figure 5A](#). The left figure shows the scale-free network fitting index  $R^2$  corresponding to different soft thresholds; the red horizontal line represents the correlation coefficient of 0.9, and the right figure represents the average network connectivity corresponding to each  $\beta$  value. A total of 19 gene modules were identified using the dynamic cutting method ([Figure 5B](#)). The number of genes contained in each gene module is shown in [Figure 5C](#), among which the blue module contained the largest number of genes, 5261 in total; the orange module contained the least number of genes, 62 in total; and the grey module indicates that the 25 genes did not aggregate into any other modules. The correlation between the two modules is shown in [Figure 5D](#), and that between gene expression and modules is shown in [Figure 5E](#). The correlation between traits and modules is shown in [Figure 5F](#), in which the modules with highly positive correlations with the traits is blue modules, and the gene of the blue module was

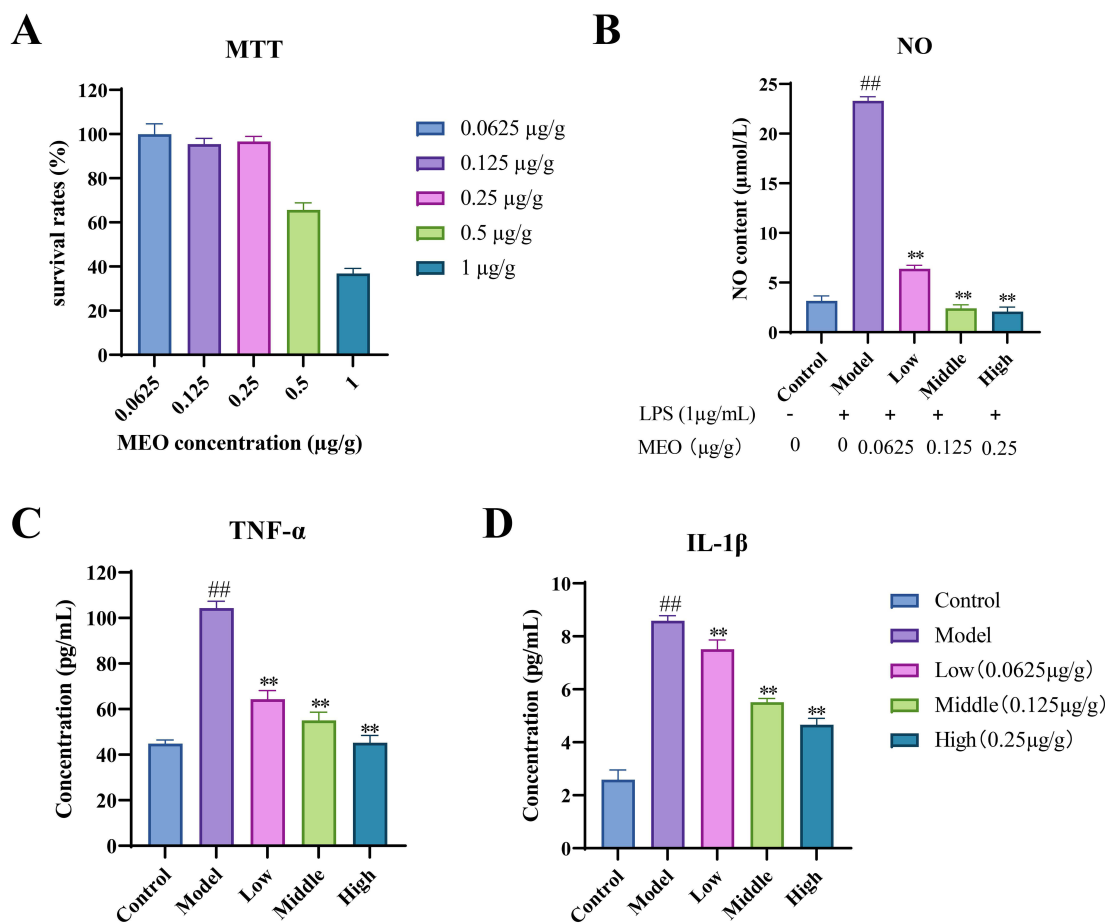


**Figure 2** The effect of MEO on cell viability in RAW264.7 macrophages. **(A)** Cell viability was measured by MTT cell viability assay. **(B)** Effect of MEO on NO production in LPS-induced RAW264.7 macrophages. **(C)** Effect of MEO on TNF- $\alpha$  production in RAW264.7. **(D)** Effect of MEO on IL-1 $\beta$  production in RAW264.7. **Notes:** ### $p$ < 0.01 vs control group. \*\* $p$ < 0.01 vs model group.

imported into the R software. KEGG enrichment analysis was performed, and 336 pathways were found to be enriched; the specific pathway results are shown in Figure 5G. Among them, the MAPK signaling pathway is located in the sixth position, which indicates that this pathway is important for the treatment of colitis with MEO.

## Component–Target Network Analysis of MEO

A total of 568 targets were de-duplicated for MEO, 25941 targets were de-duplicated for colitis, and 2500 DEGs were obtained using the Omicsmart platform. The intersection targets of the three genes were identified using the Venny2.1.0 platform; and 71 key targets of MEO for colitis treatment were obtained (Figure 6A). By importing the data into Cytoscape 3.7.1, we obtained a component–target network diagram of MEO for colitis (Figure 6B), where blue represents the intersection targets and orange represents the active components. The STRING platform was used to construct a PPI network diagram using the intersecting targets, the results are presented in Figure 6C.

## Reordered KEGG Enrichment Analysis After Introducing Weighting Coefficients

71 intersecting targets were imported into the R software for KEGG enrichment analyses. In total, 17 enrichments were identified by KEGG pathway analysis (Figure 6D). After introducing weighting coefficients, the order of KEGG pathways was changed, and the results are shown in Figure 6E. The results revealed that the MAPK signaling pathway had a higher rank (from 7 to 6). Bai et al<sup>46</sup> suggest MAPK is a key pathway in colitis treatment; therefore, this pathway may be important for treating colitis using MEO.



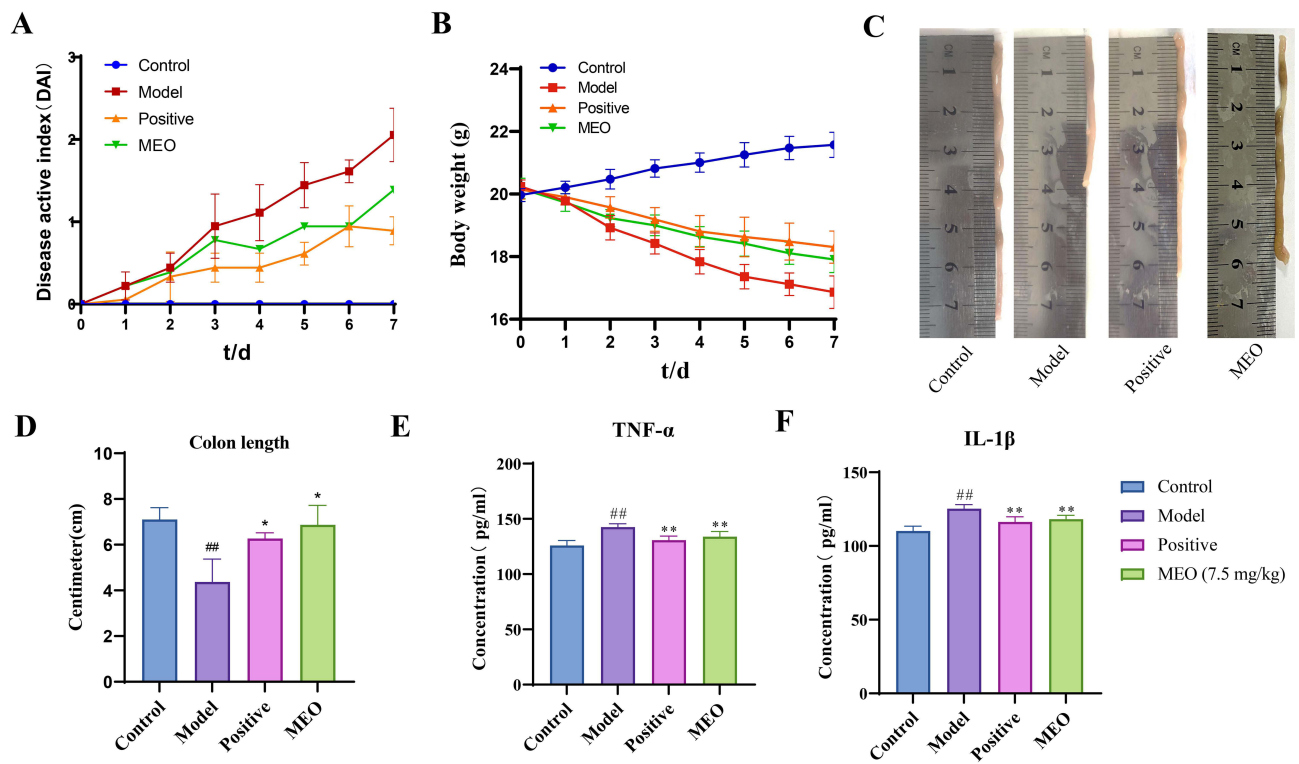


**Figure 3** The DAI, colon morphology and serum levels of TNF- $\alpha$  and IL-1 $\beta$  in colitis mice. **(A)** DAI scores. **(B)** Changes in the body weight in each group. **(C)** Morphological analysis of the colon in each group. **(D)** Differences in colon length in each mice group. **(E)** The levels of TNF- $\alpha$  in colon tissues of colitis mice. **(F)** The levels of IL-1 $\beta$  in colon tissues of colitis mice. **Notes:** ## $P < 0.01$  vs control group. \* $P < 0.05$ , \*\* $P < 0.01$  vs model group.

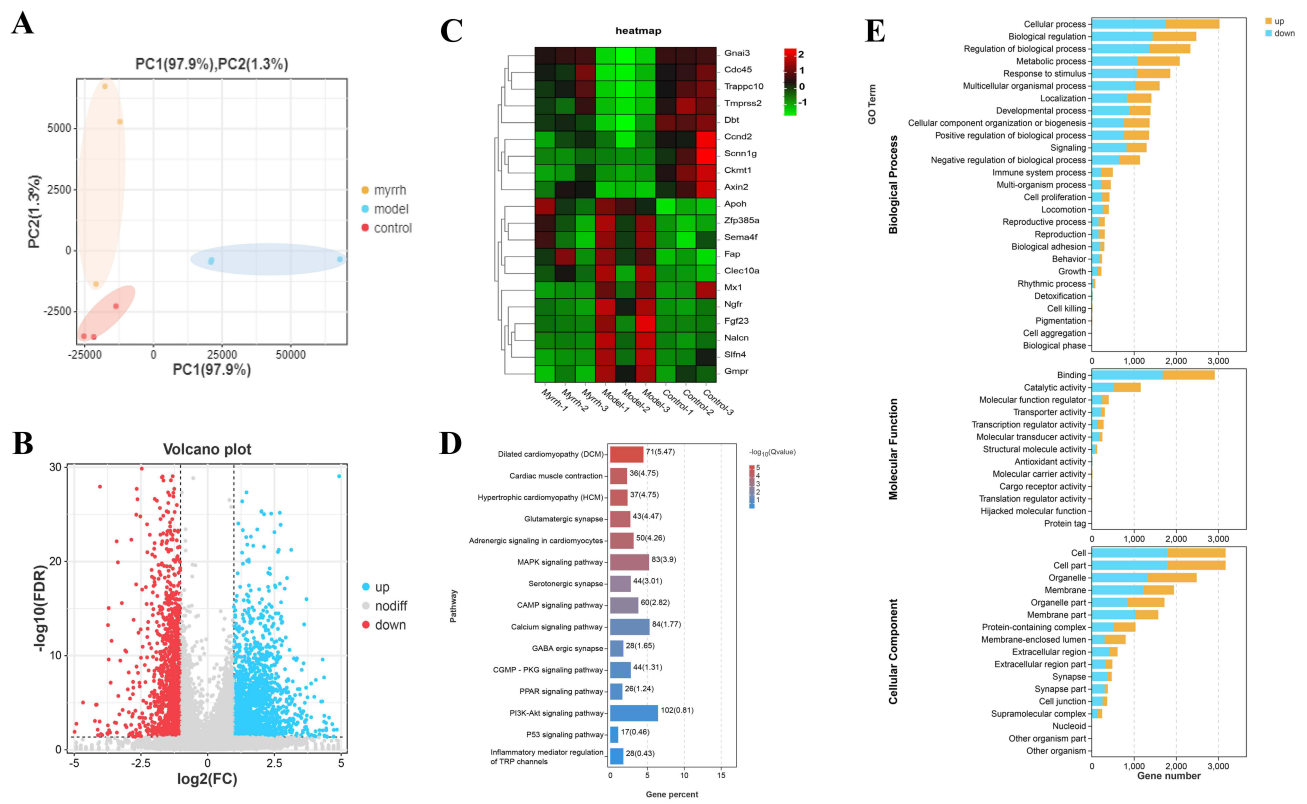


**Figure 4** Results of RNA-seq analysis in colitis mice with MEO. **(A)** PCA graph. **(B)** Volcano graph. **(C)** Heat map of DEGs. **(D)** KEGG enrichment results. **(E)** GO enrichment results.

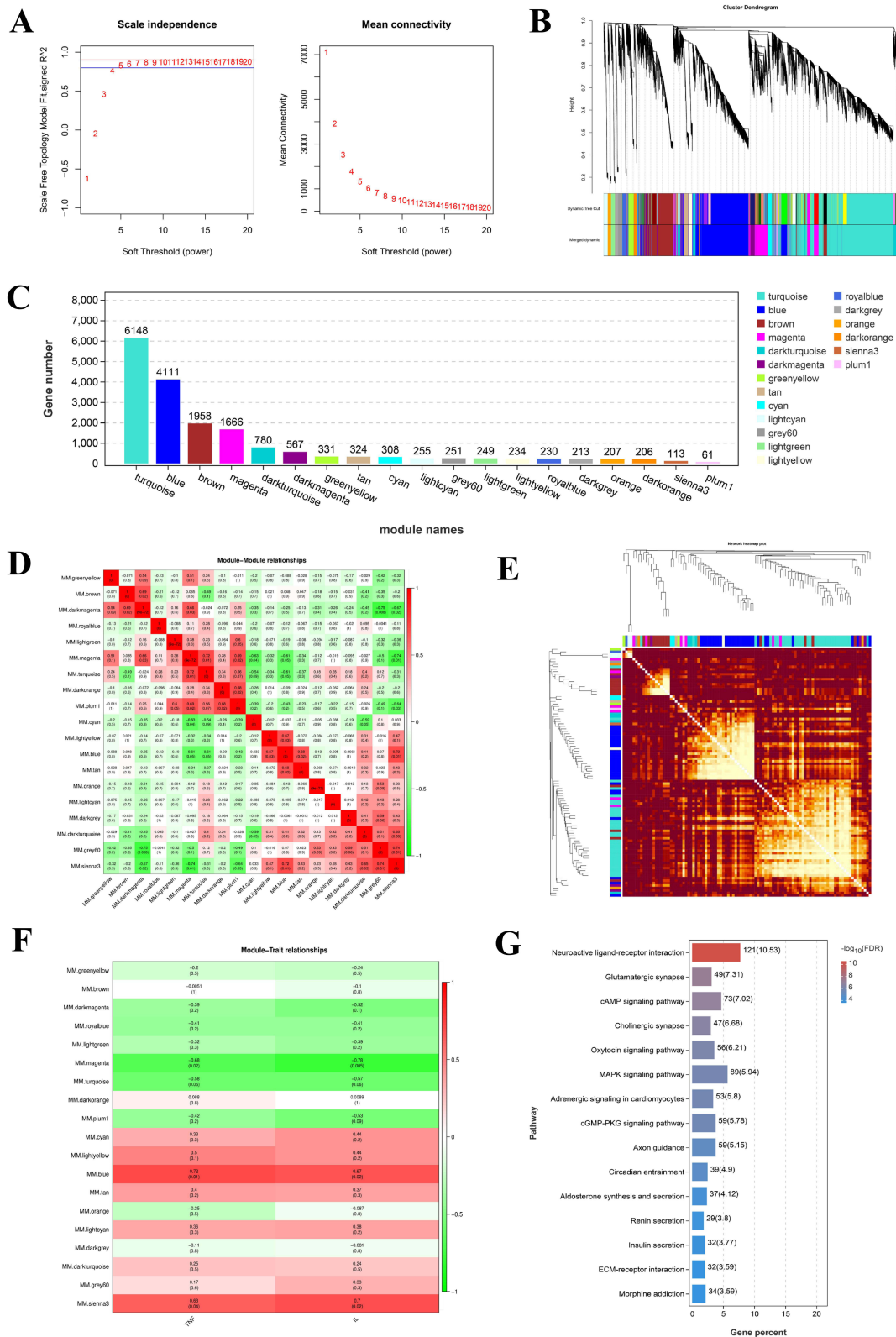


**Figure 5** Results of WGCNA. (A) Selection of the soft threshold value. (B) Gene clustering tree and module division. (C) Gene number distribution in each module. (D) Heat map for correlation analysis between two modules. (E) Heat map of gene expression and inter-module correlation analysis. (F) Results of correlation analysis of trait modules. (G) KEGG results enriched by the blue modules.

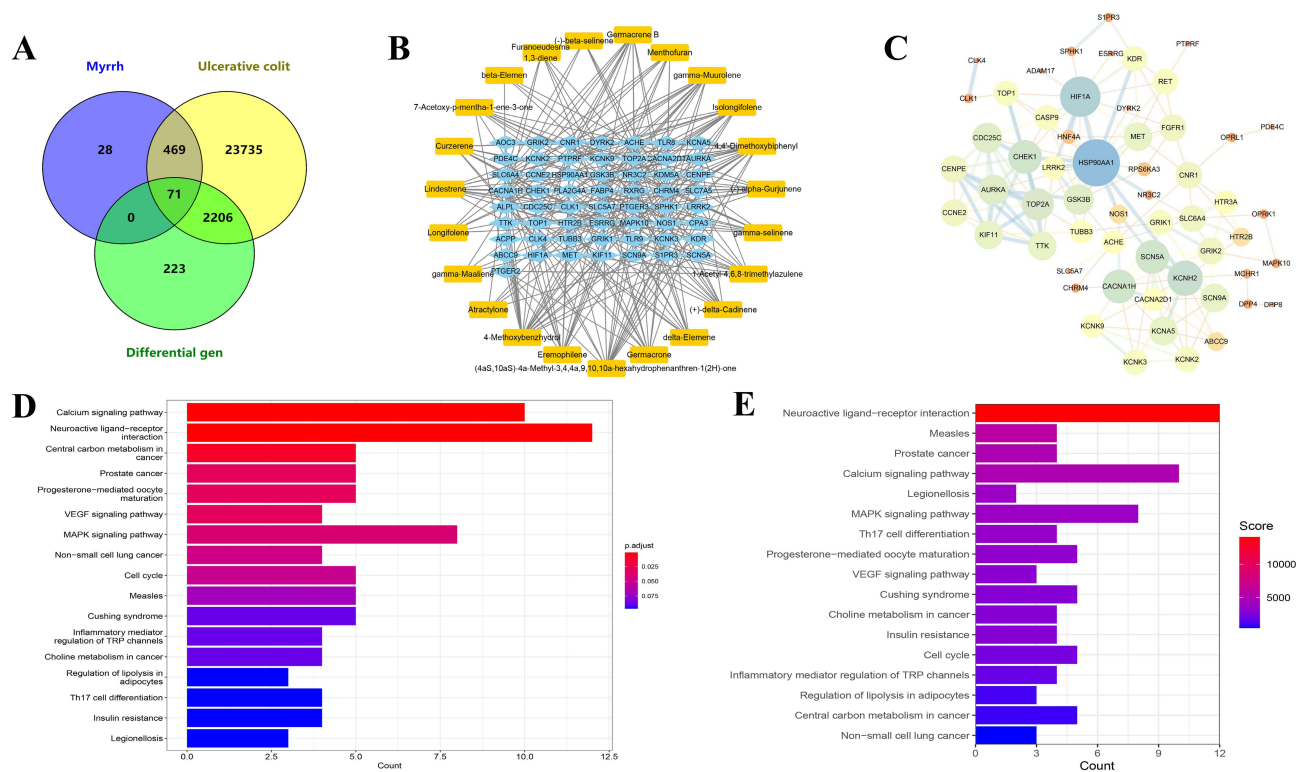


**Figure 6** The results of MEO component–target network analysis and KEGG pathway enrichment analysis. **(A)** Intersection map of MEO targets, ulcerative colitis targets, and DEGs. **(B)** Component–target map of MEO. **(C)** PPI network map of the key targets. **(D)** KEGG enrichment analysis before introducing weighting coefficients. **(E)** KEGG enrichment analysis after introducing weighting coefficients.

## Molecular Docking Results

Molecular docking of the key targets CACNA2D1, RAS, ERK, and JNK in the MAPK pathway. Gabapentin, Sotorasib, Acetylsalicylic acid, and Halicin were selected as specific ligands for the corresponding targets and were evaluated based on their binding energy scoring scores. The results are presented in Figure 7 and Table 3. The results showed that gamma-Murololene, Curzerene, beta-Elementene, and Furanoeudesma 1.3-diene components had higher scores than the specific ligands. Therefore, we can presume that these four active components of MEO play pivotal roles in colitis treatment.

## DAI and Colon Morphology in Colitis Mice

The body weight of mice in the control group gradually increased. The model and MEO groups of mice had loose or even diluted feces and severe weight loss on the third day after modeling, and blood in the stool on the fourth day. However, the symptoms of mice in the MEO group started to improve on the fifth day, with a gradual increase in body weight and improved stool properties. Figure 8A and B) illustrates the changes in DAI scores and body weights of the mice in each group. These results indicated that MEO can effectively relieve colitis in mice. The colons of mice in the model group were short in length, and the mucous membrane was congested and swollen, whereas the colons of mice in the MEO group were longer. Images of the colons of each mouse group are shown in Figure 8C, and the differences in colon length are shown in Figure 8D.

## Effects of Different MEO Doses on Serum TNF- $\alpha$ and IL-1 $\beta$ Levels

The results are shown in Figure 9A and B. The serum TNF- $\alpha$  and IL-1 $\beta$  ( $P < 0.0001$ ) levels were significantly higher in the model group. Furthermore, TNF- $\alpha$  and IL-1 $\beta$  levels were greatly decreased to different degrees in the MEO group ( $P < 0.01$ ).

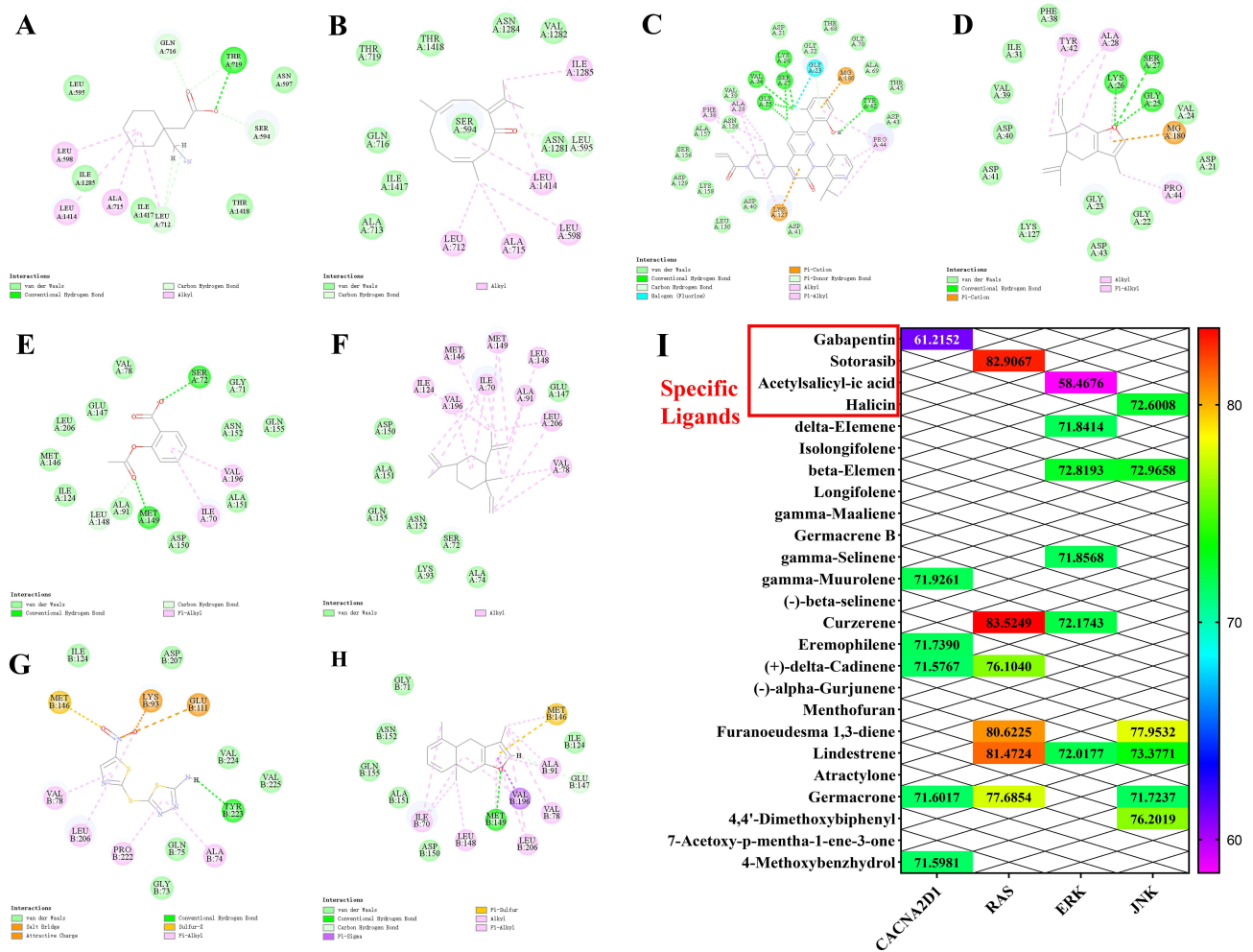


**Figure 7** Molecular docking and thermogram results of the key targets with active components and specific ligands. (A) the docking results of 7mix protein of CACNA2D1 target with the specific ligand Gabapentin. (B) the docking results of 7mix protein of CACNA2D1 target with the gamma-Muurolene component. (C) the docking results of 3kkq protein of RAS target with the specific ligand Sotorasib. (D) the docking results of 3kkq protein of RAS target with the Curzerene component. (E) the docking results of 2okI protein of ERK target with the specific ligand Acetylsalicylic acid. (F) the docking results of 2okI protein of ERK target with the beta-Elemene component. (G) the docking results of 3v6r protein of JNK target with the specific ligand Halicin. (H) the docking results of 3v6r protein of JNK target with the Furanoedesma 1.3-diene component. (I) the heat map of molecular docking.

## HE Staining Results

The HE staining results of the colon tissue of mice are shown in Figure 9C. The intestinal tissues of mice in the control group had a basic normal structure. The model group showed obvious abnormalities with a large number of inflammatory cells infiltrating the tissue. The high-dose group was normal with a small amount of inflammatory cell

**Table 3** The Docking Scores of Key Targets with Active Components and Specific Ligands

Key Target	Active Components	Docking Score	Specific ligands	Docking Score
CACNA2D1	gamma-Muurolene	71.9261	Gabapentin	61.2152
CACNA2D1	Eremophilene	71.739		
CACNA2D1	Germacrone	71.6017		
CACNA2D1	4-Methoxybenzhydrol	71.5981		
CACNA2D1	(+)-delta-Cadinene	71.5767		

(Continued)

**Table 3** (Continued).

Key Target	Active Components	Docking Score	Specific ligands	Docking Score
RAS	Curzerene	83.5249	Sotorasib	82.9067
RAS	Lindestrene	81.4724		
RAS	Furanoedesma 1,3-diene	80.6225		
RAS	Germacrone	77.6854		
RAS	(+)-delta-Cadinene	76.104		
ERK	beta-Elemene	72.8193	Acetylsalicylic acid	58.4676
ERK	Curzerene	72.1743		
ERK	Lindestrene	72.0177		
ERK	gamma-Selinene	71.8568		
ERK	delta-Elemene	71.8414		
JNK	Furanoedesma 1,3-diene	77.9532	Halicin	72.6008
JNK	4,4'-Dimethoxybiphenyl	76.2019		
JNK	Lindestrene	73.3771		
JNK	beta-Elemene	72.9658		
JNK	Germacrone	71.7237		

infiltration and no necrosis. These results suggested that the high-dose MEO group had better inhibitory effects against colitis.

### Immunohistochemical Analysis

The results are shown in **Figure 10A** large number of positive cells was observed in the colon tissues of the model group. The area of positive staining in colon tissues was reduced to varying degrees in the MEO group. Our results suggest that MEO effectively reduced the expression of p-JNK, p-ERK, and TNF- $\alpha$  in colon tissues.

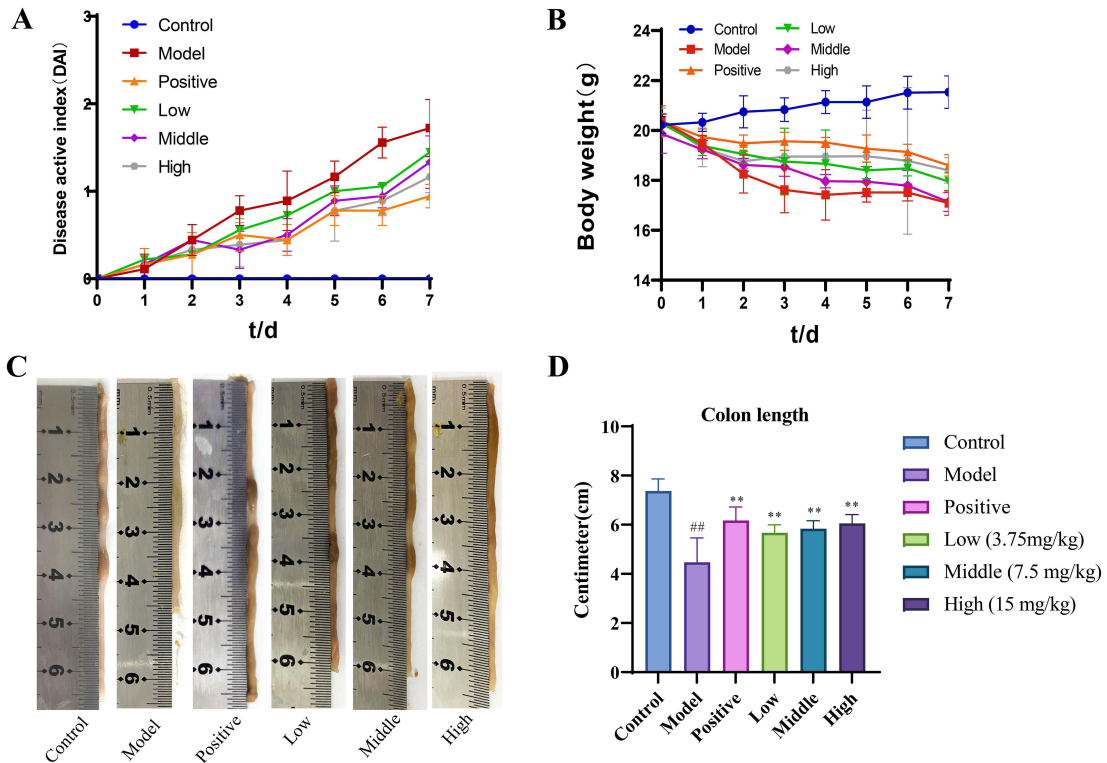


**Figure 8** The DAI score and colon morphology in colitis mice. **(A)** DAI scores. **(B)** Changes in the body weight of in each group. **(C)** Morphological analysis of the colon in different group. **(D)** Differences in colon length in each mice group.  $^{##}P < 0.01$  vs control group. **Note:**  $^{**}P < 0.01$  vs model group.



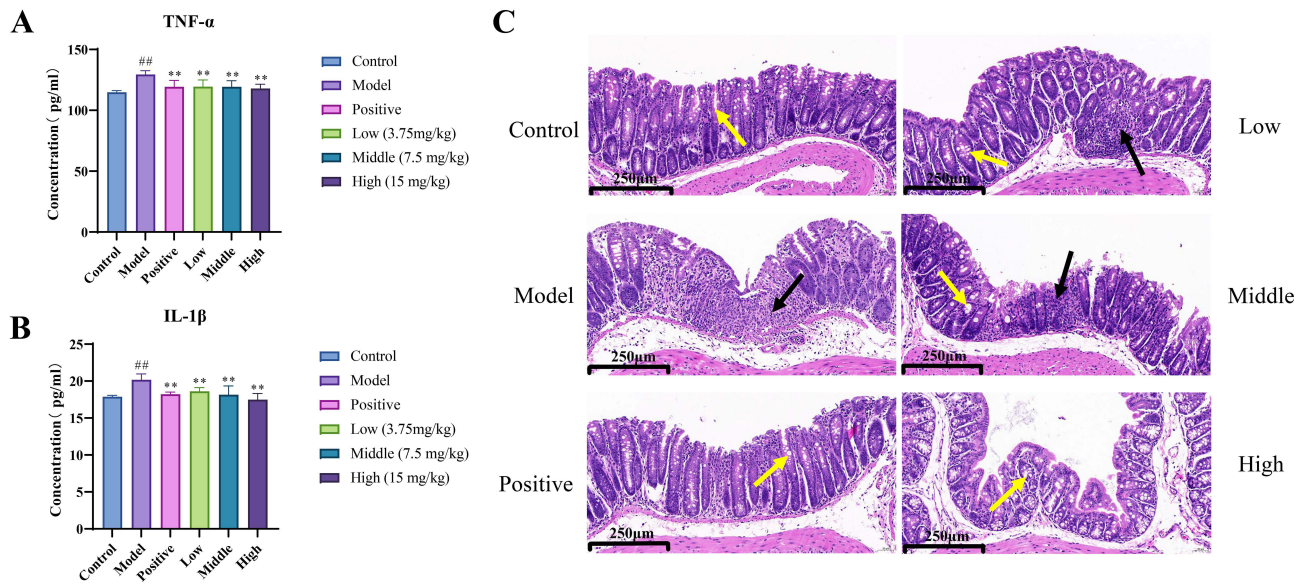


**Figure 9** The Results of MEO inhibition of serum inflammatory factor levels and effects on colonic histopathology in colitis mice. **(A)** Serum TNF-α levels of each mice group. **(B)** Serum IL-1β levels of each mice group. **(C)** Effect of MEO on DSS-induced histopathological changes in the colon. The yellow arrows show goblet cells in the normal colon, and the black arrow indicates inflammatory infiltration. **Note:** <sup>\*\*</sup>*P* < 0.01 vs model group, <sup>##</sup>*P* < 0.01 vs control group.

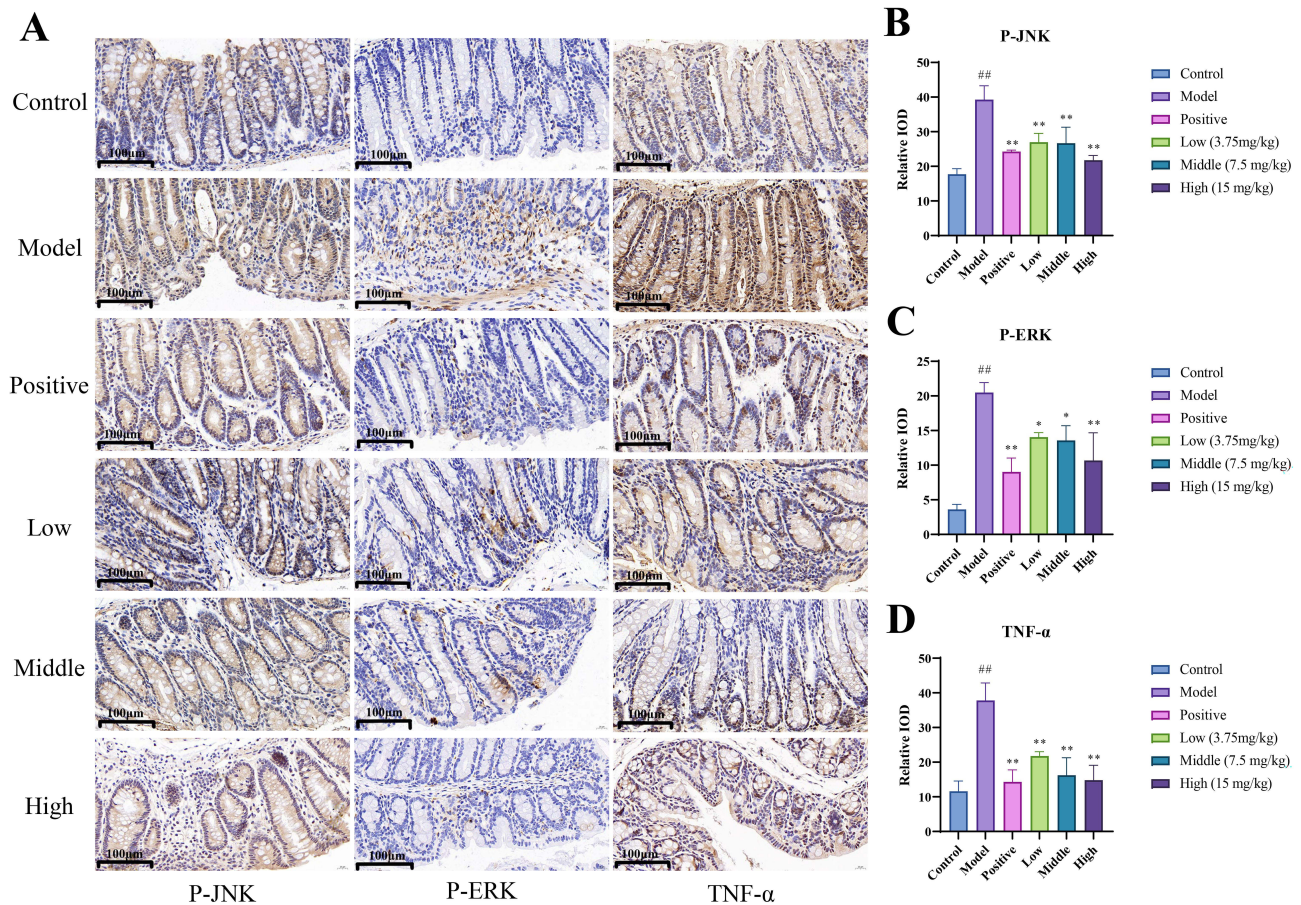


**Figure 10** The Results of Immunohistochemistry. **(A)** Effect of MEO on the levels of p-JNK, p-ERK, and TNF-α protein in DSS-induced colon tissues. **(B)** Protein levels of p-JNK in colon tissues of each mice group. **(C)** Protein levels of p-ERK in colon tissues of each mice group. **(D)** Protein levels of TNF-α in colon tissues of each mice group. **Note:** <sup>##</sup>*P* < 0.01 vs control group, <sup>\*</sup>*P* < 0.05, <sup>\*\*</sup>*P* < 0.01 vs model group.



## Western Blot Results

The results showed that, the levels of p-JNK, JNK, p-ERK, and ERK were significantly higher in model group ( $P < 0.01$ ). However, the levels decreased in the MEO group ( $P < 0.05$ ), and the effect was similar to that in the positive group. Taken together, the results suggest that MEO can effectively inhibit the activation of the MAPK signaling pathway in the colon after DSS induction; the results are shown in Figure 11.

## Discussion

In this study, *in vitro* experiments were conducted to determine the anti-inflammatory effects of MEO on LPS-induced RAW264.7 macrophages. It was found that MEO can reduce the levels of NO, TNF- $\alpha$ , and IL-1 $\beta$ . Subsequently, *in vivo* experiments established a DSS-induced colitis mouse model, and DAI scores showed that high doses of MEO were more effective. The transcript levels of TNF- $\alpha$  and IL-1 $\beta$  were significantly reduced in colitis mice after high-dose MEO administration, which inhibited the colitis inflammatory response to some extent. Western blot was performed and the results showed that the protein expression of p-JNK and p-ERK was most reduced in the high dose group of MEO. We hypothesize that MEO may reduce inflammation by inhibiting the activation of the MAPK signaling pathway, thereby ameliorating colitis in mice.

Many studies have indicated that the mechanisms involved in anti-colitis effects include the MAPK-mediated pathway, JAK/STAT3 pathway, P13k/Akt pathway, and NF- $\kappa$ B pathway. Gao et al<sup>47</sup> suggest that the serum p-ERK and p-JNK levels were significantly increased in a DSS mouse model, and the MAPK signaling pathway was successfully activated. These findings indicate that the MAPK pathway may play a crucial role in colitis pathogenesis. In addition, growing evidences showed that the pathogenesis of colitis is related to MAPK signaling cascade.<sup>48,49</sup> When the transmembrane receptor CACN on the cell membrane receives an external signal stimulus, it releases Ca<sup>2+</sup> and transmits them to RasGRP, which exchanges GDP for GTP, thereby activating Ras. After Ras activation, it recruits and activates downstream oncogene Raf. The activated Raf gradually stimulates MEK1/2 and activates ERK1/2. Among them, ERK participates in and mediates inflammatory responses, regulates inflammatory factor production, promotes epithelial cell proliferation and differentiation, and inhibits apoptosis of small intestinal epithelial cells.<sup>50</sup> Simultaneously, RAS indirectly activates JNK protein through the activation of MEKK and MKK.<sup>51</sup> It has been shown that JNK is a key mediator in most pathological signaling pathways of IBD. In the colon of IBD patients, JNK activity is significantly elevated, significantly increasing susceptibility to bacterial components and cytokines.<sup>52</sup> It binds to the transcription factor AP-1 (oncogene transcription factor), leading to AP-1 activation and release of a large number of inflammatory factors such as TNF- $\alpha$  and IL-6,<sup>53,54</sup> thus exacerbating the progression of colitis disease.

Molecular docking of the key targets CACNA2D1, RAS, ERK, and JNK in the MAPK signaling pathway with their specific ligands and active components in MEO revealed that gamma-Muuroleone, Curzerene, beta-Elementene, and Furanoedesma 1.3-diene may be key components associated with the MAPK pathway-based therapeutic effect of MEO in colitis.

By performing WGCNA analysis of differentially expressed genes in mice, 19 gene modules were obtained by dynamic cleavage, and TNF- $\alpha$  and IL-1 $\beta$  trait data were correlated with each module to derive the module with the most significant positive correlation. Genes in the modules were enriched in KEGG pathway analysis. The combined analysis

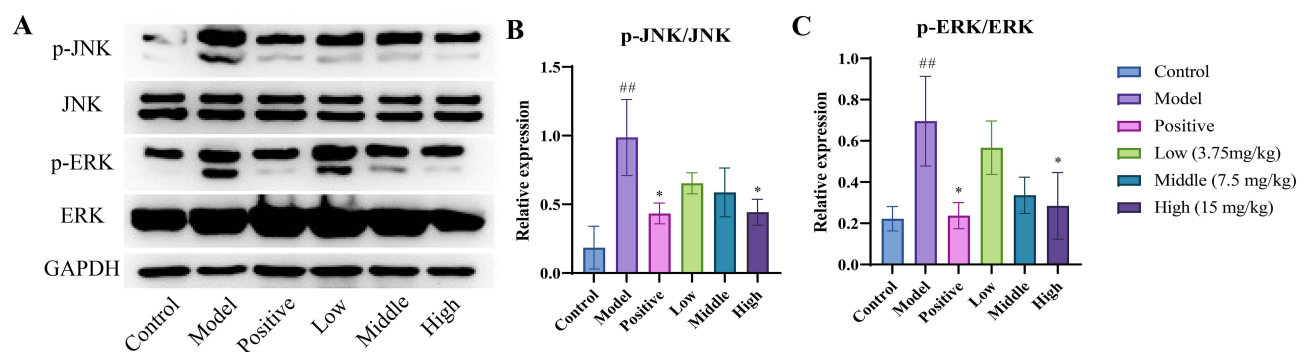


**Figure 11** The results of Western blot. (A) Changes in the levels of P-JNK, JNK, P-ERK, and ERK in DSS-induced colon tissues after treatment with MEO. (B) Protein levels of p-JNK/JNK in colon tissues of each mice group. (C) Protein levels of p-ERK/ERK in colon tissues of each mice group. Notes: ## $P < 0.01$  vs control group. \* $P < 0.05$  vs model group.

of transcriptome sequencing results, WGCNA analysis, and KEGG pathway analysis after the introduction of weighting coefficients showed that the MAPK signaling pathway ranked high, ranked 5th in transcriptome KEGG enrichment results and ranked 6th in WGCNA analysis, especially after the introduction of weighting coefficients ranked from 7th to 6th, so we considered it to be an important pathway of MEO against colitis.

In this study, we found that the therapeutic mechanism of colitis may be MEO acts on the CACN transmembrane transporter protein CACNA2D1 through its gamma-Muurolene component, which reduces  $\text{Ca}^{2+}$  influx and attenuates RAS activation. Simultaneously, Curzerene directly acts on RAS, further inhibiting its activity. In a cascade reaction, the inhibition of phosphorylated RAS (p-RAS) reduces the activation of downstream Raf and MEK. MEK is a dual-specificity kinase, and its inhibited activity simultaneously weakens the activation of ERK1 and ERK2.<sup>55</sup> The  $\beta$ -elemene component in MEO binds to ERK, reducing the levels of p-ERK, which in turn decreases the phosphorylation of transcription factors such as c-Fos and c-Jun in the cell nucleus. It is well known that c-Fos and c-Jun together form heterodimers to form the transcription factor complex AP-1, which promotes the proliferation and differentiation of epithelial cells and inhibits apoptosis in small intestinal epithelial cells.<sup>56</sup> Meanwhile, the inhibition of RAS activation leads to decreased MEKK1 activity, due to the high selectivity of MEKK1 to MKK4 in vivo, the content of phosphorylated MKK4 decreases sharply, which ultimately leads to the decrease in the downstream p-JNK level.<sup>57</sup> In addition, Furanoedesma 1.3-diene in MEO acts directly on JNK and reduces p-JNK activity. These two aspects simultaneously decrease the number of downstream AP-1 binding proteins and inhibit the MAPK signaling pathway, resulting in a decrease in the production of  $\text{TNF-}\alpha$  and  $\text{IL-1}\beta$ ,<sup>58</sup> which reduces the incidence of colon injury, improves the colon condition, and alleviates colitis.

In summary, we used weighting coefficients combined with network pharmacology methods to predict the mechanism of action of MEO on colitis, which was validated by pharmacodynamic experiments. The results indicated that the mechanism of MEO for colitis may involve the interaction of  $\gamma$ -Muurolene, Curzerene,  $\beta$ -Elemene and Furanoedesma 1.3-Diene components with CACNA2D1, RAS, ERK and JNK targets, thereby inhibiting the expression of p-ERK and p-JNK in the MAPK pathway. The mechanism of which is shown in Figure 12. Nonetheless, our study exhibits many

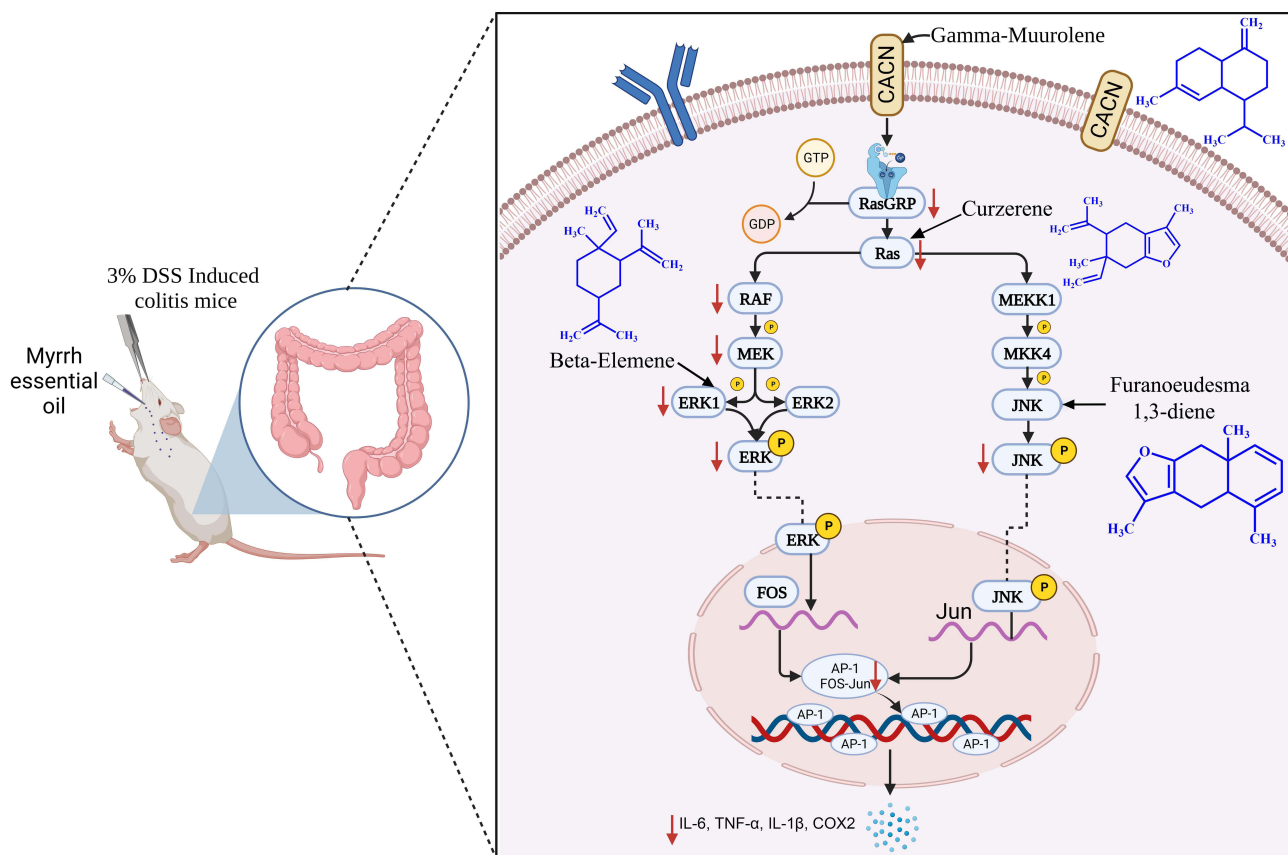


**Figure 12** The mechanism of MEO in the treatment of colitis through the MAPK pathway.

shortcomings. Although our research has made some progress, there are some limitations. Multiple pathways were enriched by network pharmacology methods, but only verified the MAPK signaling pathway, and did preliminary mechanistic studies and pharmacodynamic evaluation of this pathway, without considering the relationship between other signaling pathways and colitis. In addition, monomeric anti-inflammatory pharmacodynamic studies should be performed for the four active components  $\gamma$ -Muurokene, Curzerene,  $\beta$ -Elemene and Furanouedesma 1.3-Diene derived from molecular docking to verify the specific anti-inflammatory effects of each MEO component.

## Conclusions

In this study, we found that MEO exhibited the protective effect against DSS-induced colitis in mice and inhibited the expression of inflammatory factors by LPS in RAW264.7 cells. Pharmacodynamic experiments revealed that MEO inhibited the release of inflammatory factors by regulating p-ERK and p-JNK in the MAPK signaling pathway through  $\gamma$ -Muurokene, Curzerene,  $\beta$ -Elemene, and Furanouedesma 1.3-diene, thereby alleviating colitis symptoms. This indicates that MEO therapy for colitis operates through a multi component, multi-target, and multi-pathway, which provides a reference for future studies on the use of MEO to treat inflammation, and provides a new idea for the subsequent development of new anti-colitis drugs.

## Abbreviations

MEO, myrrh essential oil; DSS, dextran sulfate sodium; RNA-seq, RNA Sequencing; WGCNA, Weighted gene co-expression network analysis; GC-MS, Gas chromatography-mass spectrometry; DAI, disease activity index; MAPK, mitogen-activated protein kinase; TNF- $\alpha$ , tumor necrosis factor- $\alpha$ ; IL-1 $\beta$ , interleukin-1 $\beta$ ; JNK, c-Jun amino-terminal kinase; p-JNK, phosphorylated amino-terminal protein kinase; ERK, extracellular signal-regulated kinase; p-ERK, phosphorylated-ERK; NO, Nitric oxide; LPS, Lipopolysaccharide; ELISA, Enzyme-linked immunosorbent assay; OB, oral bioavailability; NIST, National Institute of Standards and Technology; RI, retention index; DMEM, Dulbecco's modified eagle medium; FBS, Fetal Bovine Serum; MTT, 3-(4,5-dimethylthiazol-2-yl)-2,5-diphenyl tetrazolium bromide; OD, optical density; SPF, Specific-pathogen-free; DEGs, differentially expressed genes; GO, Gene Ontology; KEGG, Kyoto Encyclopedia of Genes and Genomes; PPI, protein-protein interaction; HE, Hematoxylin-eosin; HRP, horseradish peroxidase; BCA, Bicinchoninic Acid Assay; GAPDH, glyceraldehyde-3-phosphate dehydrogenase.

## Ethics Statement

All laboratory operations on Animals follow the Guidelines for the Care and Use of Laboratory Animals published by the National Research Council and published by the National Institutes of Health. This study was approved by the Animal Ethics Committee of the Shaanxi University of Traditional Chinese Medicine for the humane care of animals (approval number SUCMDC20220530003). GeneCards, Online Mendelian Inheritance in Man (OMIM), DisGeNET and Comparative Toxicogenomics Database (CTD) are public databases that allow unlimited reuse under open licenses, and the study did not carry out clinical trial research, so it's to be exempt from ethical review.

## Acknowledgments

The authors gratefully acknowledge the financial supports by Shaanxi Provincial Traditional Chinese Medicine Administration (ZYJXG-Y23005); Shaanxi Provincial University Youth Innovation Team of Aromatic Chinese Medicine Industrialization Key Technology; Project of Shaanxi Provincial Department of science and technology (2023-YBSF-474); Shaanxi University of Traditional Chinese Medicine National Fund Incubation Project (2021GP29); Inner Mongolia Autonomous Region Science and Technology Program (2022YFSH0001); National Key Research and Development Program of China (2023YFD1600402, 202YFD1600403, 2021YFD1601004); Xi'an Science and Technology Programme (2023JH-JSJQ-0007); Project of Shaanxi Provincial Administration of Traditional Chinese Medicine (2021-PY-005); Scientific Research Program Funded by Education Department of Shaanxi Provincial Government (23JP034); Key Discipline of High Level Traditional Chinese Medicine in Shaanxi Province, Traditional Chinese Medicine Processing; Shaanxi Provincial Engineering Research Center for Traditional Chinese Medicine Pieces;

Shaanxi University Engineering Research Center of Chinese Medicine Aromatic Industry. We thank Bullet Edits Limited for linguistic editing and proofreading of the manuscript.

## Author Contributions

All authors made a significant contribution to the work reported, whether that is in the conception, study design, execution, acquisition of data, analysis and interpretation, or in all these areas; took part in drafting, revising or critically reviewing the article; gave final approval of the version to be published; have agreed on the journal to which the article has been submitted; and agree to be accountable for all aspects of the work.

## Disclosure

Fengyun Bai and Ying Sun were employed by Shaanxi Dongtai Pharmaceutical Co., Ltd. The authors report no other conflicts of interest in this work.

## References

- Ungaro R, Mehandru S, Allen PB, Peyrin-Biroulet L, Colombel J-F. Ulcerative colitis. *Lancet*. 2017;389(10080):1756–1770. doi:10.1016/s0140-6736(16)32126-2
- Yu YR, Rodriguez JR. Clinical presentation of Crohn's, ulcerative colitis, and indeterminate colitis: symptoms, extraintestinal manifestations, and disease phenotypes. *Semin Pediatr Surg*. 2017;26(6):349–355. doi:10.1053/j.sempedsurg.2017.10.003
- Park SC, Jeon YT. Current and emerging biologics for ulcerative colitis. *Gut Liver*. 2015;9(1):18–27. doi:10.5009/gnl14226
- Yang ZH, Jia ZJ, Suo FY, Zhu XR, Yao SK. Study on the mechanism of Huanglian jiedu decoction in the treatment of ulcerative colitis based on network pharmacology. *Mod J Integr Traditional Chinese and Western Med*. 2022;31(03):359–367. doi:10.3969/j.issn.1008-8849.2022.03.013
- Xu JB. *LncRNA Mediate Macrophage Activation and the Repairing Effect of Compound Essential Oils on Its Inflammation Under PM2.5 Exposure*. Master. Dalian Medical University; 2020.
- Kuck K, Unterholzner A, Lipowicz B, et al. Terpenoids from myrrh and their cytotoxic activity against HeLa Cells. *Molecules*. 2023;28(4):1637. doi:10.3390/molecules28041637
- Cao B, Wei XC, Xu XR, et al. Seeing the unseen of the combination of two natural resins, frankincense and myrrh: changes in chemical constituents and pharmacological activities. *Molecules*. 2019;24(17):3076. doi:10.3390/molecules24173076
- Wang Y, Zhao Y, Chen Y, Pan G, Jia X. Extraction of chemical components of myrrh using SFE-CO<sub>2</sub> and GC-MS analysis. *Chin Traditional Herbal Drugs*. 2005;1:821–823.
- Younis NS, Mohamed ME. Protective effects of myrrh essential oil on isoproterenol-induced myocardial infarction in rats through antioxidant, anti-inflammatory, Nrf2/HO-1 and apoptotic pathways. *J Ethnopharmacol*. 2021;270:113793. doi:10.1016/j.jep.2021.113793
- Zhou Y, Ouyang W. Preparation of myrrh essential oil nanoemulsion and its anti-inflammatory effects study. *Animal Husb Veter Med*. 2012;44(S1):348–349.
- Yang B, Chen ZC, Chen FY, Bian YT, Huang WM, Luo YM. Research progress in chemical constituents and biological activities of myrrh. *J Chinese Med Mater*. 2021;44(10):2476–2484. doi:10.13863/j.issn1001-4454.2021.10.042
- Ha RW, Zhou HY, Bai Y, Wang QQ, Zhan ZL, Wang H. Chemical components of myrrh: A review. *Modern Chin Med*. 2022;24(07):1374–1386. doi:10.13313/j.issn.1673-4890.20210201002
- Su S, Wang T, Duan JA, et al. Anti-inflammatory and analgesic activity of different extracts of Commiphora myrrh. *J Ethnopharmacol*. 2011;134(2):251–258. doi:10.1016/j.jep.2010.12.003
- Tipton DA, Lyle B, Babich H, Dabbous MK. In vitro cytotoxic and anti-inflammatory effects of myrrh oil on human gingival fibroblasts and epithelial cells. *Toxicol in vitro*. 2003;17(3):301–310. doi:10.1016/s0887-2333(03)00018-3
- Haffor AS. Effect of Commiphora molmol on leukocytes proliferation in relation to histological alterations before and during healing from injury. *Saudi J Biol Sci Apr*. 2010;17(2):139–146. doi:10.1016/j.sjbs.2010.02.007
- Shen T, Li GH, Wang XN, Lou HX. The genus Commiphora: a review of its traditional uses, phytochemistry and pharmacology. *J Ethnopharmacol*. 2012;142(2):319–330. doi:10.1016/j.jep.2012.05.025
- Holleran G, Scaldaferrri F, Gasbarrini A, Currò D. Herbal medicinal products for inflammatory bowel disease: a focus on those assessed in double-blind randomised controlled trials. *Phytother Res*. 2020;34(1):77–93. doi:10.1002/ptr.6517
- Novoselov VV, Sazonova MA, Ivanova EA, Orekhov AN. Study of the activated macrophage transcriptome. *Exp Mol Pathol*. 2015;99(3):575–580. doi:10.1016/j.yexmp.2015.09.014
- Wang Y, Zou J, Jia Y, et al. The mechanism of lavender essential oil in the treatment of acute colitis based on "quantity-effect. *Weight Coeffi NetPharma Fron Pharma*. 2021;12:644140. doi:10.3389/fphar.2021.644140
- Li X, Ma LN, Guo LW, et al. Analysis of gene co-expression network related to rice blast resistance using WGCNA method. *Molecu Plant Breed*. 2022;20(12):3950–3958. doi:10.13271/j.mpb.020.003950
- Langfelder P, Horvath S. WGCNA: an R package for weighted correlation network analysis. *BMC Bioinf*. 2008;9(1):559. doi:10.1186/1471-2105-9-559
- Gao R, Shu W, Shen Y, et al. Sturgeon protein-derived peptides exert anti-inflammatory effects in LPS-stimulated RAW264.7 macrophages via the MAPK pathway. *Journal of Functional Foods*. 2020;72:104044. doi:10.1016/j.jff.2020.104044
- Ren D, Wang P, Liu C, et al. Hazelnut protein-derived peptide LDAPGHR shows anti-inflammatory activity on LPS-induced RAW264.7 macrophage. *Journal of Functional Foods*. 2018;46:449–455. doi:10.1016/j.jff.2018.04.024
- Maines LW, Fitzpatrick LR, French KJ, et al. Suppression of ulcerative colitis in mice by orally available inhibitors of sphingosine kinase. *Dig Dis Sci Apr*. 2008;53(4):997–1012. doi:10.1007/s10620-007-0133-6



25. Huang S, He J, Chen Y, et al. Effect of huangqin decoction on regulating intestinal flora in colitis mice characterized as inhibition of the NOD2-dependent pathway. *Pharm Biol.* 2021;60(1):108–118. doi:10.1080/13880209.2021.2017981
26. Lin Y, Su J, Wang M, Li Y, Zhao Z, Sun Z. Hypericum sampsonii attenuates inflammation in mice with ulcerative colitis via regulation of PDE4/PKA/CREB signaling pathway. *J Ethnopharmacol.* 2022;296:115447. doi:10.1016/j.jep.2022.115447
27. Zheng Y, Liang C, Li Z, et al. Study on the mechanism of Huangqin Decoction on rats with ulcerative colitis of damp-heat type base on mtDNA, TLR4, p-PI3K, p-Akt protein expression and microbiota. *J Ethnopharmacol.* 2022;295:115356. doi:10.1016/j.jep.2022.115356
28. Fu B, He S. Transcriptome analysis of silver carp (*Hypophthalmichthys molitrix*) by paired-end RNA sequencing. *DNA Research.* 2012;19(2):131–142. doi:10.1093/dnares/dsr046
29. An W, Huang Y, Chen S, et al. Mechanisms of rhizoma coptidis against type 2 diabetes mellitus explored by network pharmacology combined with molecular docking and experimental validation. *Sci Rep.* 2021;11(1):20849. doi:10.1038/s41598-021-00293-8
30. Wu T, Hu E, Xu S, et al. clusterProfiler 4.0: a universal enrichment tool for interpreting omics data. *Innovation.* 2021;2(3):100141. doi:10.1016/j.xinn.2021.100141
31. Li GX, Wang SJ, Huo J. Identification of differentially expressed genes particularly associated with immunity in uremia patients by bioinformatic analysis. *Anal Cell Pathol.* 2022;2022:5437560. doi:10.1155/2022/5437560
32. Gustavsson EK, Zhang D, Reynolds RH, Garcia-Ruiz S, Ryten M. ggtranscript: an R package for the visualization and interpretation of transcript isoforms using ggplot2. *Bioinformatics.* 2022;38(15):3844–3846. doi:10.1093/bioinformatics/btac409
33. Song X, Zhang Y, Dai E, Wang L, Du H. Prediction of triptolide targets in rheumatoid arthritis using network pharmacology and molecular docking. *Int Immunopharmacol.* 2020;80:106179. doi:10.1016/j.intimp.2019.106179
34. Wang J, Chang H, Su M, et al. The potential mechanisms of cinobufotalin treating colon adenocarcinoma by network pharmacology. *Front Pharmacol.* 2022;13:934729. doi:10.3389/fphar.2022.934729
35. Mariguela V, Chacha S, Cunha AA, Troncon L, Zucoloto S, Figueiredo L. Cytomegalovirus in colorectal cancer and idiopathic ulcerative colitis. *Rev Inst Med Trop Sao Paulo.* 2008;50(2):83–87. doi:10.1590/s0036-46652008000200004
36. So T, Ishii N. The TNF-TNFR family of co-signal molecules. *Adv Exp Med Biol.* 2019;1189:53–84. doi:10.1007/978-981-32-9717-3\_3
37. Varfolomeev E, Vucic D. Intracellular regulation of TNF activity in health and disease. *Cytokine.* 2018;101:26–32. doi:10.1016/j.cyto.2016.08.035
38. Cui X, Jin Y, Hofseth AB, et al. Resveratrol suppresses colitis and colon cancer associated with colitis. *Can Prev Res.* 2010;3(4):549–559. doi:10.1158/1940-6207.Ccrp-09-0117
39. Lee SH, Kwon JE, Cho ML. Immunological pathogenesis of inflammatory bowel disease. *Intest Res.* 2018;16(1):26–42. doi:10.5217/ir.2018.16.1.26
40. Natsui M, Kawasaki K, Takizawa H, et al. Selective depletion of neutrophils by a monoclonal antibody, RP-3, suppresses dextran sulphate sodium-induced colitis in rats. *J Gastroenterol Hepatol.* 1997;12(12):801–808. doi:10.1111/j.1440-1746.1997.tb00375.x
41. Souza RF, Caetano MAF, Magalhaes HIR, Castelucci P. Study of tumor necrosis factor receptor in the inflammatory bowel disease. *WORLD J GASTROENTEROL.* 2023;29(18):2733–2746. doi:10.3748/wjg.v29.i18.2733
42. Bajzät D, Kéri AF, Imrei M, et al. Safety analysis of preoperative anti-TNF- $\alpha$  therapy in pediatric IBD after intestinal resection: a systematic review and meta-analysis. *INFLA BOW DIS DEC 5.* 2023;29(12):1971–1980. doi:10.1093/ibd/izac274
43. Wang JW, Kang GB, Lu HY, et al. Novel bispecific nanobody mitigates experimental intestinal inflammation in mice by targeting TNF- $\alpha$  and IL-23p19 bioactivities. *CLINI TRANS MED.* MAR 2024;143:e1636. doi:10.1002/ctm2.1636
44. He J, Shao JH, Wang LY, Wang F. Research of astragalus polysaccharide on ulcerative colitis in rats. *The Chinese J Clin Pharmacol.* 2022;38(14):1678–1682. doi:10.13699/j.cnki.1001-6821.2022.14.023
45. Singh KK, Gupta A, Bharti C, Sharma H. Emerging techniques of Western blotting for purification and analysis of protein. *Future J Pharm Sci.* 2021;7(1):1. doi:10.1186/s43094-021-00386-1
46. Bai XS, Bai G, Tang LD, Li Y, Huan Y, Wang H. MiR-195 alleviates ulcerative colitis in rats via MAPK signaling pathway. *Eur Rev Med Pharmacol Sci.* 2020;24(5):2640–2646. doi:10.26355/eurrev\_202003\_20533
47. Gao Z, Yu C, Liang H, et al. Andrographolide derivative CX-10 ameliorates dextran sulphate sodium-induced ulcerative colitis in mice: involvement of NF-kappaB and MAPK signalling pathways. *Int Immunopharmacol.* 2018;57:82–90. doi:10.1016/j.intimp.2018.02.012
48. Arthur JS, Ley SC. Mitogen-activated protein kinases in innate immunity. *Nat Rev Immunol.* 2013;13(9):679–692. doi:10.1038/nri3495
49. Li D, Xie T, Guo T, et al. Sialic acid exerts anti-inflammatory effect through inhibiting MAPK-NF-kB/AP-1 pathway and apoptosis in ulcerative colitis. *Journal of Functional Foods.* 2023;101:105416. doi:10.1016/j.jff.2023.105416
50. Yu L, Yan J, Sun Z. D-limonene exhibits anti-inflammatory and antioxidant properties in an ulcerative colitis rat model via regulation of iNOS, COX-2, PGE2 and ERK signaling pathways. *Mol Med Rep.* 2017;15(4):2339–2346. doi:10.3892/mmr.2017.6241
51. Oh Y-T, Yue P, Zhou W, et al. Correction: oncogenic ras and B-raf proteins positively regulate death receptor 5 expression through co-activation of ERK and JNK signaling. *J Biol Chem.* 2020;295(26):8870. doi:10.1074/jbc.AAC120.014435
52. Roy PK, Rashid F, Bragg J, Ibdah JA. Role of the JNK signal transduction pathway in inflammatory bowel disease. *World J Gastroenterol.* 2008;14(2):200–202. doi:10.3748/wjg.14.200
53. Xue Y, Shao CC, Duan LX, et al. Oncostatin M promotes hepatic progenitor cell activation and hepatocarcinogenesis via macrophage-derived tumor necrosis factor-alpha. *Cancer Lett.* 2021;517:46–54. doi:10.1016/j.canlet.2021.05.039
54. Simion V, Zhou H, Pierce JB, et al. LncRNA VINAS regulates atherosclerosis by modulating NF-kB and MAPK signaling. *JCI Insight.* 2020;5(21). doi:10.1172/jci.insight.140627
55. Wei FX, Xie YY, He LZ, Tao LJ, Tang DM. ERK1 and ERK2 kinases activate hydroxyurea-induced S-phase checkpoint in MCF7 cells by mediating ATR activation. *CELL SIGNAL JAN.* 2011;23(1):259–268. doi:10.1016/j.cellsig.2010.09.010
56. Huang C, Dong J, Cheng L, et al. Alkaloids from aconitum carmichaelii alleviates DSS-induced ulcerative colitis in mice via MAPK/NF-kappaB/STAT3 signaling inhibition. *Evid Based Complement Alternat Med.* 2022;2022:6257778. doi:10.1155/2022/6257778
57. Zheng T, Zhang B, Chen C, et al. Protein kinase p38 $\alpha$  signaling in dendritic cells regulates colon inflammation and tumorigenesis. *Proc Natl Acad Sci U S A.* 2018;115(52):E12313–E12322. doi:10.1073/pnas.1814705115
58. Xu Y, Nowrangi D, Liang H, et al. DKK3 attenuates JNK and AP-1 induced inflammation via kremen-1 and DVL-1 in mice following intracerebral hemorrhage. *J Neuroinflammation.* 2020;17(1):130. doi:10.1186/s12974-020-01794-5

Journal of Inflammation Research

Dovepress

## Publish your work in this journal

The Journal of Inflammation Research is an international, peer-reviewed open-access journal that welcomes laboratory and clinical findings on the molecular basis, cell biology and pharmacology of inflammation including original research, reviews, symposium reports, hypothesis formation and commentaries on: acute/chronic inflammation; mediators of inflammation; cellular processes; molecular mechanisms; pharmacology and novel anti-inflammatory drugs; clinical conditions involving inflammation. The manuscript management system is completely online and includes a very quick and fair peer-review system. Visit <http://www.dovepress.com/testimonials.php> to read real quotes from published authors.

Submit your manuscript here: <https://www.dovepress.com/journal-of-inflammation-research-journal>